

Dear Editor,

We are happy to submit a revised version of the manuscript 'Estimating real driving emissions from MAX-DOAS measurements at the A60 motorway near Mainz, Germany' (amt-2020-125).

The issues raised by the referees have been addressed in our authors' responses provided on AMTD and have been accounted for in the revised version of the manuscript.

We provide an updated version of the manuscript, as well as a version with tracked-changes in order to expose the modifications we made. The most important changes of the revised manuscript are:

- The date of the measurement day was added explicitly in abstract and conclusion.
- The impact of integration time on the results was discussed in more detail.
- Uncertainties induced by cloud cover were accounted for in the retrieval of the measured NO₂ SCD caused by traffic emissions.
- The CAABA-MECCA simulation of road traffic was reworked and a Gaussian dispersion model was applied analysing the effects of ozone titration and turbulence on the NO_x to NO₂ ratio. Here, an additional section was added to the Appendix (Sect. C1).
- Sect. 3.5 Comparison to the HBEFA database was added comparing emission factors given by the database to our measurements. Real Driving Emission conformity factors are discussed in the previous comparison to the European emission standards.
- The settings of the spectral analysis have now been transferred to a Table. An exemplary fit result was added to the Appendix.
- In the Figures, the labels for the MAX-DOAS instruments were changed and in Fig. 4, panel (E) was dropped.
- For correlation between the inverse wind velocity and the traffic induced NO₂ signal, the non-averaged version (previously Fig. A4) was omitted.

Kind regards,

Bianca Lauster

Attachments:

- Authors' response to Referee comment #1
- Authors' response to Referee comment #2
- Revised version of the manuscript with tracked-changes

Reply to comments from Referee #1

We would like to thank the referee for the comprehensive and thoughtful review, and helpful comments which are addressed individually in the response below. The reviewer's comments are included in italics with the responses in blue.

The study by Lauster et al. describes a new method to quantify the NO_x emissions from a motorway using two MAX-DOAS in parallel. This method is new and complementary to the existing ones, the analysis appears valid, and the presentation of the results in the paper is in general clear, although there is room for improvement in this respect. The experiment also addresses a hot topic regarding air quality. This work fits well in the scope of AMT. Therefore this work should be published, once the authors have taken into account the following remarks.

Major points:

One limitation of this study is its small database. To my understanding, there was only one day of measurements (10 May 2019). This date appears in the main text only in section 3 (I know it is in the caption of Fig. 1). It is fine to demonstrate a new technique with a small database, but this should be clear in the text. That means adding the date of experiment to the sentences of the abstract and conclusion which gives the factor 11±7. In case the authors performed more of such measurements but could only use those of May 10 for some reasons, it would be interesting to (briefly) explain what the problems were.

We have added the date to the respective sentences in abstract and conclusion. Also, we added (l. 39 in the revised manuscript):

"The presented results are based on one day of measurements (10 May 2019) for proof of concepts. Further measurements could then be used to analyse, e.g., different driving conditions in more detail."

Indeed, we only have one measurement day with this setup (including weather station and using this viewing geometry). The primary aim of our study is to present a proof of concept of the measurement method. Further studies could then include different measurement conditions (e.g. weekdays vs. weekend, different seasons) as well as additional measurement sites to investigate different driving conditions (e.g. speed limits, slope of the motorway). Such an extensive study, however, is beyond the scope of this manuscript.

It's confusing that the legends indicate 'west side', 'east side' in Fig. 2 and Fig. A1, since they show measurements when both instruments were on the west side to record reference measurements. I suggest to label the instruments e.g. A and B across the text and figures instead (keeping the west side, east side where it makes sense).

We see the point and adapted the legends and the text accordingly.

l. 125 and below: Can the authors explain why they use the non filtered SCDtraffic estimate in the main text, if they have filtered the clouds in A2? Does the statement that the 'clouds have only a small impact' refer to the 16% of A2? If so, this is more important than the standard error of the mean (5%) and thus not 'a small impact'.

In the main text, we refer to the unfiltered case as no clear relation between the cloudiness and the NO₂ signal is seen. However, we agree to the referee that a more accurate error estimation should include the deviation of 16%. We therefore added this deviation as an additional error to the traffic induced NO₂ SCD and the following processing steps. Also, we dropped the sentence that “clouds have a small impact” (I.132) to avoid further confusion. In the end, the additional error has no significant effect on the outcome of the emission estimation.

I.177: 'Our simulations with CAABA confirm...' -> The O3 concentration is indeed an important parameter in the NO₂/NO evaluation, one can imagine that the atmospheric mixing is as well. Could the authors add a figure with these simulations, e.g. in the appendix? If the NO₂/NO ratio is stable in the O3 conditions on 10 May 2019 in Mainz, it is interesting to know in which O3 conditions this ratio is not stable.

We thank the referee for this important comment. Indeed we did not yet consider the titration of ozone close to the source, where NO concentrations are very high and ozone becomes depleted. This will stop further conversion of NO to NO₂. However, turbulent mixing with ambient air increases with distance from the source. Thereby, ozone in the emitted air parcel is replenished and the oxidation of NO continues.

In the revised version of the manuscript, we apply a Gaussian dispersion model using Pasquill stability classes (Pandis and Seinfeld, 2006) based on the atmospheric stability on the measurement day. With this dispersion model we estimate the extent of the emission plume and derive the NO₂ mixing ratio from our measurements. While turbulence induced by the local topography and obstacles like trees is neglected, it helps to estimate the evolution of NO₂ mixing ratio between emission source and measurement location. From the comparison of the dispersion model and the observations, we conclude that the ozone-limited chemical regime only prevails very close to the emission source.

In order to consider this in our emission estimate calculation, we subdivide the transport of the air parcel in two sections: 1) Close to the emission source we assume that only negligible amounts of NO are converted into NO₂ and no further conversion takes place as ozone is depleted. 2) Turbulent mixing with ambient air refills the ozone reservoir and NO to NO₂ conversion can be described by the CAABA model simulations. For simplicity, we chose the distance at which the initial NO₂ mixing ratio of CAABA model simulations is reached as the transition between both sections.

As the new approach shortens the time for NO to NO₂ conversion, it is found that the NO₂/NO_x ratio is smaller than assumed in the previous approach without considering ozone limitations. Since both approaches yield the same results within the error estimation, a modification of the given NO₂/NO_x ratio was not deemed necessary.

The revised approach is described in the text (I. 195 and Appendix C1 in the revised manuscript) including a figure to the simulations.

I. 188 The authors could refer to previous experiments which indicate that it is unlikely that the NO₂/NO equilibrium would be reached so close to a source, e.g. the airborne measurements of NO_x fluxes from power plants (see for instance the Phd of A. Meier, Uni. Bremen), or similar studies.

We have added (in I.214 of the revised manuscript):

“However, it is rather unlikely that the equilibrium state is reached so close to the emission source (as also found for airborne measurements of emission fluxes from power plants; Meier, 2018).”

Similar to other studies, the NO/NO₂ emission rate only stabilises at a distance of 3-5 km from the source. Therefore, we do not expect to measure the equilibrium state already at a distance of a few hundred metres. But from our simulations we can conclude that a large part of the emitted NO was already converted to NO₂.

In appendix A1, the statement 'As for cloud free condition a constant CI is expected' is misleading since the CI varies, even without any clouds, with the sun position (see e.g. Gielen, 2014). In practice, this statement is only valid because of the short considered time period, please rephrase.

Agreed and changed to “An almost constant CI is expected for cloud free conditions in this time period.”

The last sentence of the appendix 'a constant wind is advantageous for the measurements' is an important take-home message and should be explicit in Sect 3.2 and in the conclusions.

Agreed and added in I.173 and I.293 of the revised manuscript.

I have several smaller suggestions to improve the presentation, see below.

Minor points:

I.8: 'independent' -> independently ?

Done.

I.13: 'A large fraction of the global emissions' -> can the authors be quantitative on this fraction? 'Therefore'-> does not seem an appropriate adverb here since it's not linked by cause to the previous sentence, what about 'Moreover'?

According to the 5th assessment report of the IPCC (2013), the anthropogenic emissions of NO_x account for approximately three-quarters of the global NO_x emissions. The phrase reads now “About three-quarters of the global emissions of NO_x originate from anthropogenic sources (IPCC, 2013).” In the next sentence, “Therefore” was changed to “Moreover”.

I.30: 'need to convert NO into NO2 as they directly measure the exhaust plume'-> can the author briefly explain why? (the emissions are mainly NO?). It makes sense to detail also since the reference is in German.

The paragraph was revised, focusing more on the general approaches used in other studies. Thereby, this sentence dropped out. The study by Pöhler and Engel (2019) internally measures NO₂, but as they directly measure the exhaust plume mainly NO (which is produced in the combustion process) is present in the sample. Therefore, the sampled NO is converted into NO₂ before the measurement.

I.55: 'the differential SCD yields the integrated tropo concentration of a specific trace gas'. This seems too short to be accurate. Please specify that the integration is along the photon path and that this quantity is relative (differential) to the column in the reference spectrum.

Agreed and rephrased more detailed. It reads now:

“Then, the differential SCD yields the integrated tropospheric concentration of a specific trace gas along the photon path (for an altitude range from the surface up to about 2 to 3 km; Frieß et al., 2019, and references therein), i.e. the column density relative to the reference spectrum.”

I.68: perpendicular -> almost perpendicular?

Done.

I. 71: 'Possible source of NOx' although that may seem obvious to the authors, I suggest to add that 'since no fire was detected in the area' for other readers

We have added “since no other sources (e.g. fires) were detected in the area”.

Spectral analysis: presenting the DOAS fit parameters (window, cross-sections, polynomial orders...) in a dedicated table would be more readable and synthetic.

Done.

I. 98: 'As can be seen in the grey area' -> actually not much can be seen in the grey area due to the y-axis scale of the lower subplot. I suggest to redo this figure 2, with the second subplot zoomed in the time period of the grey area so that we really see that the delta is about $4e14$. This would also make the subplots less redundant.

Thanks for this suggestion. We changed the plot accordingly.

In the text, the authors should also explain what this delta is in practice (interpolated? one channel assumed constant?) since the measurements do not appear synchronized in time.

It is correct that the measurements are not ideally synchronised in time. Therefore, to obtain the difference between the two instruments, the time series of one instrument was interpolated onto the time axis of the other. A corresponding sentence was added to the manuscript (l. 106 in the revised manuscript).

I. 104 'spectra are being integrated' -> '... averaged' ?

We have changed this to „accumulated“.

I. 285 'as shown in fig.2'-> 'fig. A2'?

We have changed “90° measurements as shown in Fig. 2” to “90° measurements (compare to Fig. 2)” as we refer to the same 90° measurements for which the NO₂ results are depicted in Fig. 2.

I. 292 'in Fig. A3 where the dashed line indicates ... threshold' -> Fig A2 ?

Thanks for pointing this out. We mixed up the sentences. It is now corrected to the following:

“The reference was inferred by fitting a 2nd order polynomial to the data and is depicted as dashed line. The filtered time series are displayed in Fig. A3.”

I. 112 It's expected that the error trends follows the RMS, as it is expected that the RMS decreases with increasing integration times. Please add a few words on the physical explanation (shot noise ...)

We have changed the following sentence

“Although the average RMS decreases for longer integration times, the NO₂ retrieval yields the same result regardless of the integration time.”

to

“For the short integration times of our measurements, the spectral residual of the fit is dominated by photon shot noise. This is also clearly demonstrated by the observed dependence of the RMS (and the fit error) on integration time. The RMS decreases for longer integration times as the ratio of the photon shot noise to the measured signal increases. In contrast to the fit error decreasing with integration time, the NO₂ retrieval yields the same average NO₂ DSCDs for different integration times.”

I. 115-116 'Consequently ... to resolve specific traffic event' -> Please break this sentence in two for the sake of readability

Done.

I. 160 For the sake of readability, I suggest to be more explicit with the geometric approximation of the AMF at 20° i.e. to write 2.92.

Agreed and added to the text.

Figure 4 is important and should be improved. The y axis of panels A and B should be zoomed to better see the variations and mean values. Panels E and F are redundant, the authors could only show one of them (leading to larger remaining subplots and a clearer figure).

Thanks for this suggestion. We adapted the plot and text accordingly.

I. 199 'These emission standards' -> 'the emission standards of trucks' (would be clearer for the reader)

Done.

Reply to comments from Referee #2

We would like to thank the referee for the comprehensive and thoughtful review, and helpful comments which are addressed individually in the response below. The reviewer's comments are included in italics font with the responses in blue.

The manuscript presents a new approach to derive average vehicle NO_x emissions on a motorway using passive MAX-DOAS. This method is a further adaptation / modification of emission estimates like performed with car MAX-DOAS [e.g. Ibrahim et al. 2010] or stationary MAX-DOAS for volcanoes [Galle et al. 2010]. While the basic measurement principle is similar, the setup was here adapted to the task of vehicle emission measurements.

The applied method is well described and clear. They have the potential to be established for general vehicle emission monitoring of whole fleets. The topic fits well in the scope of AMT. There are two major weak points. First, several parameters which influence the measurement are not well considered. They lead to a further increase of the derived emission factor error, which is already quite large with $4.3 \pm 2.5 \times 10^{-19}$ molec/(ms).

Second, the calculations of the expected NO_x emissions are incorrect and underestimated, which make the manuscript and likely the measurement principle disputable. This does not mean that a significant higher emission is derived than expected, but a more realistic expected emission would strengthen the value of the manuscript. The manuscript should first be corrected before publication.

Major points:

Chapter 3.4: Expected traffic emissions

The EURO emission standard is a limit which is based on a lab test cycle on a chassis dynamometer (NEFZ, and now WLTP) and only needs to be fulfilled on average over the whole test cycle. The emissions can be for some driving situations higher and for other lower. Especially on a motorway where the engine load is high, emissions are typically higher than the average especially for passenger cars (e.g. HBEFA data base, Lashkina and Lashkin 2016, Athanasios et al. 2019, for trucks e.g. TNO 2016). Second, It is expected and well known, that real driving emissions (RDE) will be higher as the driving and surrounding properties in the test cycle are not realistic (like also, mentioned in the manuscript l. 26.). For trucks this is also limited since EURO VI with a RDE factor of 1.5. This means that EURO VI trucks are allowed to emit on average $1.5 \times 460 \text{mg/kWh} = 690 \text{mg/kWh}$ in RDE (not the applied 460mg/kWh). For passenger cars the RDE confirmation factor is 2.1 since EURO-6d-Temp. RDE are thus for these diesel cars $2.1 \times 80 \text{mg/km} = 168 \text{mg/km}$. For older vehicles RDE is not tested and thus an emission confirmation with a confirmation factor is not defined. In conclusion this means that the emission standard (Table 1) are not the expected RDE even if the vehicles confirm to the emission limit. The error becomes obvious as the expected weighted emission limit of the vehicle fleet (l. 213) is with 116mg/km below the RDE limit newest EURO 6d-temp diesel passenger cars need to confirm (168mg/km). Third, there are engine situations where significant higher emissions are allowed like cold start. If directly comparing measured

emissions with calculated emissions, it should be excluded that these driving situations could contribute. Else they need to be considered.

There are different ways to handle the comparison more correctly:

a) The expected emissions are modelled using the vehicle fleet, number, driving property at the measurement site and emission RDE data from HBEFA data base. This can also be made if it is expected that all vehicles conform to the legislation or if included known RDE emission values. The expected emissions will increase in comparison to the authors calculation. That does not mean that they are than in agreement with the measurement, but this would allow a comparison between expected and measured average emissions.

b) The derived total emission is compared to the average emission limit on the chassis dynamometer (like currently done in the manuscript), however than a direct relation of how much the derived emissions are higher needs to be avoided. It must be clearly stated that the calculated emissions do not represent the expected emissions on the motorway, which is higher even if the vehicles conform to the legislation. The comparison just gives the reader a relation between the numbers. In general the manuscript would than focus more on the derived total emission and less on the comparison.

c) The calculated expected emissions are at least more realistic. That mean that emission factors for motorways need to be used. Additional the RDE conformity factor need to be applied, which however only exist for newer EURO 6 / VI. How to deal with older cars is thus difficult. Additionally some estimated emissions of the trains need to be considered. Even if they are not clearly seen in the DSCD's (like mentioned in I. 130), they are still included in these data.

First, we thank the referee for this very extensive discussion and ideas to improve the calculation of the expected/theoretical emissions of the vehicle fleet!

As the referee already points out, a more sophisticated assessment using the European emission standards and RDE conformity factors cannot be done in a consistent way as hereto the RDE conformity factors for older emission classes are missing. However, to reduce the risk of confusion we changed „expected emissions“ to „theoretical emissions“ to emphasise the fact that these values are referring to the European emission standards and not to real driving conditions.

We added a paragraph (I.227 in the revised manuscript):

“The European emission standards are theoretical values for the allowed emissions of different pollutants. They are, however, not the expected emissions under real driving conditions. In order to bring the values in line, so-called Real Driving Emissions (RDE) conformity factors are used for new emission norms (Euro 6; Council of the European Union, 2016). To avoid inconsistencies, in the following only the European emission standards serve to estimate the theoretically expected emissions.”

We also added another sentence to Sect. 2.1 Experimental setup:

“The chosen motorway section has a speed limit of 100 km h⁻¹. The next access and exit is about 1 km in one direction and 1.5 in the other direction. Acceleration and deceleration should, therefore, only have a minor effect at the measurement site.”

The measurement location is thus ideal to measure constant emission, which also encourages investigating the average emission flux over the whole measurement time series.

Additionally, we now analysed the expected emission as given by the HBEFA database. Here, we concentrated on the vehicle categories 'passenger cars' (PC) and 'heavy duty vehicles' (HDV) as these can be readily identified in the camera recordings of the motorway section. It can further be differentiated between hot/cold emission categories. However, cold starts are not to be expected on this motorway section and also they only have little impact on the overall emissions when comparing the values given by the database. We used the aggregated emission factors for NO_x (in units of g/vehkm) of the year 2020. Again comparing the values e.g. to the year 2015, differences especially in the category of HDV can be seen. In total, the effect remains rather small. Using the emission factors of the HBEFA database regarding NO_x emissions, 1.1×10^{19} molec/(m s) are to be expected on average. Our measurements show values which are 4+2 times larger than the calculated emissions. Although the database provides real driving emission factors, there remains a discrepancy to the measurements. Nonetheless, this additional comparison shows that the measurement method yields reasonable results and seems to be able to quantify average emissions of the motorway section. A respective section was added to the revised manuscript (Sect. 3.5).

I. 209: The number of total travelled distance of trucks may not represent the real truck composition on the motorway. Especially on the motorway typically more foreign trucks are present than on average on the road. A more realistic number can be found from the toll collect system

(https://www.bag.bund.de/DE/Navigation/Verkehrsaufgaben/Statistik/Mautstatistik/mautstatistik_node.html).

We agree to the referee that a considerable amount of non-German trucks has to be expected on the motorway. Analysing the data given by the German toll collect system, however, shows no significant deviation of the distribution with regard to the emission classes although roughly 35% are non-German trucks.

Chapter 2.2: Deriving DSCD's

A spectral fit is missing in the appendix.

Done.

I. 110: The given NO₂ DSCD error of 0.006×10^{16} molec cm⁻² does not agree to the given RMS values. Please provide the correct NO₂ DSCD errors of the spectral analysis. The error for the average DSCD is not reducing with Gaussian error propagation.

We have replaced "average NO₂ error" by "NO₂ fit error" and "average RMS" by "RMS" to state more clearly to what we refer. Further, we rephrased "The standard error of the average NO₂ DSCD..." to "The standard error of the mean regarding the NO₂ DSCD is about 0.006×10^{16} molec cm⁻²". The error of 0.006×10^{16} molec cm⁻² here refers to the statistical error of the NO₂ DSCD time series, whereas the RMS values (also shown in Fig. 3) are given by the QDOAS analysis and averaged over all data points.

Also in l. 125 / 126 the given error seems to be calculated with gaussian error propagation of the mean which is not valid. Systematic measurement errors do not behave like a statistical standard error.

This is correct. We calculated the statistical error in the average traffic induced NO₂ SCD using the standard error of the mean. This is a valid approach as systematic errors that impact the calculated difference between the upwind and downwind instrument would also affect the 90° reference spectra. Here, no major deviation between the instruments can be seen (Fig. 2). The fit error of the DSCDs is mainly composed of a measurement noise component and an instrument noise component. Hereby, the instrument noise is largely influenced by the integration time and shows the same trend as discussed above for the RMS. It is concluded that the measurement result is not affected by this. The measurement noise includes statistical fluctuations of the NO₂ signal and is thus also not relevant when averaging over longer time spans as done in the retrieval of the averaged, traffic induced NO₂ SCD.

A physical explanation is added (l. 117 in the revised manuscript):

“For the short integration times of our instruments, the spectral residual of the fit is dominated by photon shot noise. This is also clearly demonstrated by the observed dependence of the RMS (and the fit error) on integration time. The RMS decreases for longer integration times as the ratio of the photon shot noise to the measured signal increases. In contrast to the fit error decreasing with integration time, the NO₂ retrieval yields the same average NO₂ DSCDs for different integration times.”

The typical averaging (2s) is very short with resulting noisy NO₂ DSCD's. The authors derive an average emission factor over a longer time period. It is explained that there is no significant difference between the different time resolutions (l. 113). It is not clear which difference the authors mean here. The one for the example in Fig. 3? Or the difference for the whole SCD_traffic? Even if the difference is small, I do not understand the argument in l. 116 “to resolve specific traffic events”, as none of these events are analyzed in the manuscript. If analyzing averaged spectral data (16 s or longer) the section 2.4 and Fig. 3 can be shorten.

In l.113 we changed “result” to “average NO₂ DSCDs” such that the sentence now reads “...the NO₂ retrieval yields the same average NO₂ DSCDs for different integration times.” The following discussion of differences refers to the deviation of the average NO₂ DSCDs for different integration times separately for both instruments, but not to the traffic induced difference between the two instruments.

We stick to the original data (2 s integration time) as we do not expect any information gain/loss when averaging over longer time spans. Although we do not explicitly use the high temporal resolution, the analysis/discussion of the integration time shows that generally it is conceivable to resolve individual emission plumes, e.g. for lower traffic volume (where it might be easier to differentiate single emission plumes) or for higher workloads (at motorway sections that show higher slopes). We added this information to the respective paragraph (l.125 in the revised manuscript).

The influence of clouds is not clear through the manuscript. Clouds seem to have a large influence on the results. It is not clear if both MAX-DOAS point at 90° at the same location, why a difference in DSCD is observed?

During the 90° measurements, both instruments were positioned close to each other (less than 2 m distance). Therefore, the spatial mismatch is rather small. Nevertheless, it would be possible that one instrument already sees a cloud edge, whereas the other does not, because of small deviations of the viewing directions. More importantly, the instruments were not synchronised in time (added to l. 106 in the revised manuscript) such that there is a time shift between the measurements of both instruments which induces deviations in the DSCD for changing cloud cover. However, we find a good agreement of the two instruments for cloud-free periods.

Both should see the same cloud and thus same variation of DSCD. From Fig. 2 it looks like a systematic offset for the “East side” instrument is observed. If such small variations already cause such large difference between the instrument (east side instrument measure higher DSCD), how can you exclude that this is not the case when the instrument measure at different locations at 20°?

In the revised version of the manuscript, any offset between the two instruments is accounted for as an additional error to the retrieved traffic induced NO₂ SCD. Moreover, the effect of clouds is generally smaller for slant viewing directions (20°) compared to the zenith viewing direction. Taking the cloud-free reference spectra assures almost perfect agreement between both instruments. In this case, we do not expect and have no indication of systematic deviations.

From Fig. 2 only the measurement situation without clouds are used for the reference.

Yes, to assure that both instruments are evaluated against the same reference conditions.

The argument in l. 132. that clouds have only a small influence is not clear as Fig. A3 shows the influence also for the emission measurement. With the argument from Fig. 2 (both instrument at west side) also only data without clouds should be used for the emission analysis (like Fig. A3 instead data from Fig. 4).

In the main text, we refer to the unfiltered case as no clear relation between the cloudiness and the NO₂ signal is seen. However, we agree that the statement in l. 132 (“clouds have a small impact”) is misleading and was therefore dropped in the revised manuscript. For more accurate error estimation, we added the corresponding deviation of 16%, which might be introduced due to the cloudiness, as an additional error to the traffic induced NO₂ SCD. Recalculating the following conversion into the VCD and emission flux, it can be seen that this has no significant effect on the outcome of the emission estimation.

Are the “West side” and “East side” instrument at the same height? If not, what would be the influence on the NO₂ DSCD if they are not at the same height? Could this cause some bias in the DSCD_traffic.

There is a height difference between the two instruments of about 40 m. However, the light path is in both cases very comparable. Both instruments are set up in the same height above the surface. Therefore, no NO₂ molecules go undetected. Moreover, both instruments measure the same background because their viewing

directions are aligned parallel. Small differences in the height (above sea level) are thus negligible.

Chapter 2.2: Estimation of real driving emissions

I. 168: The vehicles emit also directly NO₂. The share is for diesel engines (the main NO_x emitters) rather high with 30%.

This is true. We added a statement in I.187 of the revised script (“Especially diesel vehicles also directly emit NO₂ (Carslaw et al., 2011, and references therein).”). For a high share of directly emitted NO₂, the equilibrium state could be reached closer to the motorway. In any case, the estimate of the equilibrium emission is within the error of the estimation following the simulation results.

I. 170: Specify that “the share of NO₂ in total NO_x” need to be known “at the measurement location”.

We have now included this information in the sentence.

I. 174: The conversion of 2/3 of NO to NO₂ is estimated to 4 minutes. This conversion needs O₃. As NO emissions are very high at the emissions source, O₃ is completely titrated, and thus NO cannot further react to NO₂. Even if the background conc. (I. 180) is at 42-44ppb, it will be zero at the motorway (like typical on high traffic roads). The further reaction requires dilution with O₃ rich air. Is this considered in the CAABA model? How this would affect the result?

We thank the referee for this important comment. Indeed we did not yet consider the titration of ozone close to the source, where NO concentrations are very high and ozone becomes depleted. This will stop further conversion of NO to NO₂. However, turbulent mixing with ambient air increases with distance from the source. Thereby, ozone in the emitted air parcel is replenished and the oxidation of NO continues.

In the revised version of the manuscript, we apply a Gaussian dispersion model using Pasquill stability classes (Pandis and Seinfeld, 2006) based on the atmospheric stability on the measurement day. With this dispersion model we estimate the extent of the emission plume and derive the NO₂ mixing ratio from our measurements. While turbulence induced by the local topography and obstacles like trees is neglected, it helps to estimate the evolution of NO₂ mixing ratio between emission source and measurement location. From the comparison of the dispersion model and the observations, we conclude that the ozone-limited chemical regime only prevails very close to the emission source.

In order to consider this in our emission estimate calculation, we subdivide the transport of the air parcel in two sections: 1) Close to the emission source we assume that only negligible amounts of NO are converted into NO₂ and no further conversion takes place as ozone is depleted. 2) Turbulent mixing with ambient air refills the ozone reservoir and NO to NO₂ conversion can be described by the CAABA model simulations. For simplicity, we chose the distance at which the initial NO₂ mixing ratio of CAABA model simulations is reached as the transition between both sections.

As the new approach shortens the time for NO to NO₂ conversion, it is found that the NO₂/NO_x ratio is smaller than assumed in the previous approach without considering

ozone limitations. Since both approaches yield the same results within the error estimation, a modification of the given NO_2/NO_x ratio was not deemed necessary. The revised approach is described in the text (l. 195 and Appendix C1 in the revised manuscript) including a figure to the simulations.

l. 178: The estimated ratio from CAABA is 0.7 +/-0.4. It is not clear which solar radiation data are used for this calculation. The same is the case for the steady state conversion factor in l. 188.

The CAABA-MECCA simulation takes the location of Mainz to calculate solar radiation at the surface using solar inclination and typical ozone and other gases' distribution in the atmosphere. It takes into account the sun's orbit on our measurement day - without clouds. Although there were scattered clouds present on the measurement day, the photolysis rates for clear sky are roughly appropriate for our measurements. The information was added to the text (l.193 in the revised manuscript).

Minor points:

Abstract: The whole approach is based on the conversion of NO to NO₂, which depends on Ozone. It is important to mention this in the abstract.

We added the following to the abstract:

“Hereto, the ozone-dependent photochemical equilibrium between NO and NO₂ is considered.”

l.7: “...concentration over the lowermost 2 to 3km.” But what is the most relevant height in such a study. The plume will not be uplifted to several 100m, but will be rather below 100m if you are so close to the highway. So this statement is confusing. What is the expected height of the plume at the “East side” location?

We have rephrased the sentence as follows:

“One major advantage of the method used here is that MAX-DOAS measurements are very sensitive to the integrated NO₂ concentration close to the surface.”

Fig. 1: Following on the plume height! How the area of highest sensitivity is calculated marked in Fig. 1?

The area of highest sensitivity indicates the area, for which our measurements have the highest sensitivity to the motorway emissions. It is estimated geometrically using the elevation angle of 20° and the estimated plume height of about 200 m. This information is now added to the text (l. 81 in the revised manuscript) and to Fig. 1.

l. 24: Since EURO 6c, the WLTP test cycle is the new test standard. For EURO VI the WHSC.

We rephrased the sentence:

“This procedure is standardised depending on the emission class, e.g. by the New European Driving Cycle (NEDC; European Parliament and Council of the European Union, 1970) and since 2017 by the Worldwide harmonized Light vehicles Test

Procedure (WLTP; Council of the European Union, 2017). These include the measurement of exhaust emissions on a chassis dynamometer.”

It should be clearer now that different test cycles are used for different emission classes. Important to note is that these test cycles make use of chassis dynamometers. Although the new test cycles are designed for more realistic driving situations, the retrieved values still cannot represent real driving conditions. The same case applies for heavy duty vehicles (World Harmonized Stationary Cycle, WHSC).

I. 30: What do you mean with “need to convert NO to NO₂” which sounds like a problem? The measurement systems observe NO_x, how the instruments measure internally NO_x is not relevant for the derived emission data.

I. 31 & I. 34: The statement “Furthermore, this approach is dependent on the exact position of the emission source and the inlet of the measuring instrument.” and “Both approaches are able to resolve the emission of individual vehicles but are depending on the wind field and the position of the exhaust pipe with respect to the measuring instrument.” is not correct. Remote sensing and plume chasing observe ratios of gases e.g. NO_x/CO₂ and derive from this the emission factor. The dilution between emission source and inlet is not relevant for the emission value. It may have an effect if a sufficient signal is captured at all, but not for the value itself. It needs to be correct that these systems directly observe RDE of individual vehicles and measurement position and wind field is not relevant.

I. 33: The statement “However, these require an estimate of the amount of primary NO₂ in the exhaust.” is only valid for older remote sensing systems, as newer directly measure also NO₂ and NO. Additionally the direct NO₂ emission is small in relation to NO, thus this error is not so large. Another reason is valid why remote sensing has large errors: The snap shot emission measurement at very specific driving conditions where these systems work are not representative for the average emissions of an individual vehicle and also not necessary on average over many measurements as many driving conditions are not covered (e.g. motorway). That would be the motivation to derive fleet average emission factors and compare it with expected emissions from models. The advantage of the described method in this manuscript over remote sensing and plume chasing is that it derives the average emission directly, where the other techniques would require a large data set.

Thanks for these comments. The paragraph was revised as follows:

“In-situ measurements such as used in vehicle chasing experiments, e.g. performed by Pöhler and Engel (2019), directly measure the exhaust plume of individual vehicles. Others use remote sensing techniques (Carshaw et al., 2011; Chen and Borken-Kleefeld, 2014) to measure exhaust gases across-road. Both approaches are able to resolve the emissions of individual vehicles but it is difficult to derive representative fleet average emission factors, e.g. to compare these with expected emissions from models, as large data sets would be required.”

Now the paragraph focuses more on the general approaches that are used for measuring emission factors without manipulating the vehicles (as e.g. for PEMS) – and less on the exact measurement techniques used in the different studies. This should also emphasise the advantage of our method as MAX-DOAS allows to measure the complete vehicle fleet without gaps/undetected emission plumes.

I. 57: If the authors state “measure the NO₂ emissions of vehicles” this would mean the direct NO₂ emissions, not including NO afterwards converted to NO₂. But the manuscript focus on NO_x emissions, derived from NO₂ DSCD.

Agreed and changed to “quantify the NO_x emissions of vehicles”.

I. 58: The background NO₂ DSCD subtraction is one of the main new methods applied in the manuscript. It should thus also be described in more detail in the method description.

Agreed and changed to “Using two MAX-DOAS instruments on the two sides of the motorway allows to measure the background NO₂ DSCDs on the upwind side and additionally the traffic induced NO₂ on the downwind side. The background NO₂ DSCD is then subtracted from the NO₂ DSCD on the downwind side and thus yields the NO₂ SCD caused by the traffic emissions.”

I. 79: The wind measurement was performed upwind, but the important wind speed of the plume is downwind. Can this be different due to shading of trees etc.? What would be the estimated error?

It is correct that the measurement of the wind field is a potential source of errors. Nevertheless, we do not expect and also have no indication of systematic differences between the two sides of the motorway. The wind data shows a rather consistent pattern throughout our measurement time series, turbulent processes in the vicinity of the motorway cannot be accounted for in this approach. We added this information to the revised manuscript in l. 166.

Chapter 2.1: Does not include the measurement date and how many measurements are performed. It looks like there was only few hours of measurements. What were the conditions during this day? Are they representative. From a statistical point of view this is a quite small data set.

We have added the date explicitly to the sentences that state the factor between measurement and theoretical emissions in the abstract and conclusion of the revised manuscript.

Also, we added (l. 39 in the revised manuscript):

“The presented results are based on one day of measurements (10 May 2019) for proof of concepts. Further measurements could then be used to analyse, e.g., different driving conditions in more detail.”

We took only one day of measurements with this setup (including weather station and using this viewing geometry). The primary aim of our study is to present a proof of concept of the measurement method. Further studies could then include different measurement conditions (e.g. weekdays vs. weekend, different seasons) as well as additional measurement sites to investigate different driving conditions (e.g. speed limits, slope of the motorway). Such an extensive study, however, is beyond the scope of this manuscript. We would still rate the conditions during the day representative for that motorway section.

The weather was sunny with broken clouds in the middle and end of the time series. Hereto, compare to Fig. A1-A3. This is also described in l.74 and in the appendix.

A more detailed description of the motorway properties is added to the manuscript (Sect. 2.1).

I. 151: The wind speed is only measured at ground level. But the landscape includes trees and hills. The wind speed may not represent the true speed of the plume. Can a better wind speed be estimated from the time shift of “West side” to “East side” of the NO₂ data (expecting that these variations are also at plume height)? An additional error for the wind at plume height should be included. What would be the influence if the wind velocity on the motorway (between the trees) is lower? Is the average wind speed derived over all wind speed data points or only in these periods when you have valid DSCD_traffic? This is even more relevant when analyzing data from Fig. A3.

We added (I.166 in the revised manuscript):

“Effects such as turbulence, especially in the vicinity of the motorway, and changing wind fields at plume height lead to uncertainties which can, however, not be readily quantified.”

There are two effects influencing the wind velocity. On the one hand, turbulence especially close to the motorway induces mixing which cannot be assessed easily. However, turbulent effects should statistically cancel out over longer time periods.

On the other hand, the wind velocity increases with height and therefore the measured NO₂ signal would be underestimated. Moreover, less NO would be converted to NO₂ as the air parcel moves faster to the downwind measurement site – again leading to an underestimation of the retrieved emission. But since the plume is confined within the lowest 200 m, this effect should be quite small.

Also, applying the cloud filter to the wind data, i.e. filtering out the same time periods as indicated by the colour index of the DOAS data, shows no significant difference (average wind velocity without cloud filter: 2.8±1.0 m/s; average wind velocity with cloud filter: 2.9±1.0 m/s).

I. 285: Here it is stated that Fig. 2 shows CI, but it shows NO₂ DSCD.

We have changed “90° measurements as shown in Fig. 2” to “90° measurements (compare to Fig. 2)” as we refer to the same 90° measurements for which the NO₂ results are depicted in Fig. 2.

I. 227: Include the applied molar mass (46,01 g/mol).

Done.

I. 244: The sentence “trucks only account for a small amount of the total traffic volume”, is confusing, as they cause a large portion of the total NO_x emissions.

We changed it to “trucks only account for parts of the total traffic volume”.

Fig. 4: A description is missing why traffic number is only shown for few times. What is with the gaps?

As stated in I.133/134, the amount of traffic was only counted over one-minute intervals on a sample basis. The bars in Fig. 4 depict the number of cars and trucks for the respective points in time.

Fig A1: Include an explanation why CI is different for both instrument even if they point both at 90° at the same location.

We added to the text (l. 331 in the revised manuscript):

„The offset of the CI between the two instruments can be ascribed to the specific instrumental properties as the instruments are not absolutely radiometrically calibrated.”

Internal properties explain the deviation of the absolute values in CI for the two instruments. However, for the analysis the respective instrument-specific reference spectrum is taken. Therefore, the outcome is not affected by different radiometric characteristics.

A3, Fig A4 and A5: The difference between the two plots is only the averaging of the data over 12min instead of 2s. The explanation why there is no correlation in A4 is hidden in l. 300. As wind speed measurements are not at the location of the plume, the correlation at the high time resolution seem to be prone for errors and confusing. I suggest directly to show only averaged data (A5), where a small time shift has only a minor effect.

We agree to the referee and removed Fig. A4 from the manuscript. The text was adapted accordingly.

Estimating real driving emissions from MAX-DOAS measurements at the A60 motorway near Mainz, Germany

Bianca Lauster¹, Steffen Dörner¹, Steffen Beirle¹, Sebastian Donner¹, Sergey Gromov¹, Katharina Uhlmannsiek¹, and Thomas Wagner¹

¹Max Planck Institute for Chemistry, Mainz, Germany

Correspondence: B. Lauster (b.lauster@mpic.de)

Abstract. In urban areas, road traffic is a dominant source of nitrogen oxides ($\text{NO}_x = \text{NO} + \text{NO}_2$). Although the emissions from individual vehicles are regulated by the European emission standards, real driving emissions often exceed these limits. In this study, two MAX-DOAS instruments on opposite sides of the motorway were used to measure the NO_2 absorption caused by road traffic at the A60 motorway close to Mainz, Germany. In combination with wind data, the total NO_x emissions for the occurring traffic volume can be estimated. Hereto, the ozone-dependent photochemical equilibrium between NO and NO_2 is considered. We show that for 10 May 2019 the measured emissions exceed the maximum expected emissions calculated from the European emission standards by a factor of 11 ± 7 . One major advantage of the method used here is that ~~from~~ MAX-DOAS measurements are very sensitive to the integrated NO_2 concentration ~~over the lowermost 2 to 3 km is determined~~ close to the surface. Thus, all emitted NO_2 molecules are detected ~~independent~~ independently from their altitude and therefore the whole emission plume originating from the nearby motorway is captured ~~by these measurements~~ which is a key advantage compared to other approaches such as in-situ measurements.

1 Introduction

Nitrogen oxides (NO_x) is a collective term for nitrogen dioxide (NO_2) and nitric oxide (NO). In the troposphere, a photochemical reaction with ozone leads to an equilibrium state between NO_2 and NO (Pandis and Seinfeld, 2006). ~~A large fraction~~ About three-quarters of the global emissions of NO_x ~~originates originate~~ from anthropogenic sources (IPCC, 2013). ~~Therefore,~~ Moreover, nitrogen oxides do not only play a major role in atmospheric chemistry but are also important in terms of air quality. The World Health Organization reports negative short-term as well as long-term exposure effects in pulmonary function and in other organs (World Health Organization et al., 2000). For this reason, the limitation of the concentration of nitrogen oxides is part of the European programme regarding ambient air quality and cleaner air (European Parliament and Council of the European Union, 2008).

Fossil fuel combustion from road traffic is a major contributor to NO_x emissions. Hence, the European emission standards were introduced to regulate the exhaust emissions of new vehicles in the EU since 1998 (European Parliament and Council of the European Union, 1998) and tightened in 2007 by a new regulation bringing into force the so-called Euro 5 and Euro 6 norms (European Parliament and Council of the European Union, 2007). New vehicles sold in the EU need to undergo a type-approval

25 procedure which verifies the compliance with these regulations. This procedure is standardised depending on the emission class,
e.g. by the New European Driving Cycle (NEDC) ~~and includes the~~ (NEDC; European Parliament and Council of the European Union, 1970
and since 2017 by the Worldwide harmonized Light vehicles Test Procedure (WLTP; Council of the European Union, 2017).
These include the measurement of exhaust emissions on a chassis dynamometer (European Parliament and Council of the European Union,

30 However, various studies (Carslaw et al., 2011; Chen and Borken-Kleefeld, 2014) have shown that the real driving conditions
are more dynamic than the tested driving cycles. In addition, it is known that several manufacturers have installed software
that manipulates the test results by reducing emissions specifically during the test procedure (Borgeest, 2017). This results in
increased exhaust emissions during normal driving operation.

In-situ measurements such as used in vehicle chasing experiments, e.g. performed by Pöhler and Engel (2019), ~~need to~~
35 ~~convert into as they~~ directly measure the exhaust plume ~~. Furthermore, this approach is dependent on the exact position of the~~
~~emission source and the inlet of the measuring instrument~~ of individual vehicles. Others use remote sensing techniques (Carslaw
et al., 2011; Chen and Borken-Kleefeld, 2014) to measure exhaust gases across-road. ~~However, these require an estimate of the~~
~~amount of primary NO₂ in the exhaust. Hence, the retrieval of the total amount of emitted NO_x is afflicted with large errors.~~
~~Moreover, the across-road method can only give a point measurement and is not necessarily representative for the average~~
40 ~~emission of a vehicle.~~ Both approaches are able to resolve the emission of individual vehicles but ~~are depending on the wind~~
~~field and the position of the exhaust pipe with respect to the measuring instrument.~~ it is difficult to derive representative fleet
average emission factors, e.g. to compare these with expected emissions from models, as large data sets would be required.

Nevertheless, in the atmosphere NO and NO₂ form an equilibrium state which is mainly influenced by the ozone con-
centration and solar irradiance but not the primary composition and amount of the exhaust gases. Thus, the Multi AXis Dif-
45 ferential Optical Absorption Spectroscopy (MAX-DOAS) yields a key advantage when operated at some distance from the
emission source. ~~The~~ This method is described in more detail in the next section. The presented results are based on one day
of measurements (10 May 2019) for proof of concepts. Further measurements could then be used to analyse, e.g., different
driving conditions in more detail.

2 Method

50 The MAX-DOAS method (Platt and Stutz, 2008) allows measuring the differential slant column density (DSCD) of different
trace gases (Hönninger et al., 2004). Hereto, spectra of scattered sunlight are recorded at different elevation angles using
ground based instruments. To convert the slant column density (SCD), which represents the integrated concentration along the
slant light path, into the vertical column density (VCD), the so-called air mass factor (AMF) is needed. For trace gas layers
close to the ground the geometric approximation for the AMF can be used (Hönninger et al., 2004). The integrated trace gas
55 concentration along the vertical path is then given by

$$\text{VCD} = \frac{\text{SCD}}{\text{AMF}} \approx \sin(\alpha) \cdot \text{SCD} \quad (1)$$

where α is the elevation angle.

In order to remove the Fraunhofer lines, the logarithm of a so-called Fraunhofer reference spectrum with preferably minimal trace gas absorption is subtracted from the logarithm of the measured spectra. To fulfil this criterion, the reference spectrum is usually recorded with an elevation angle $\alpha = 90^\circ$, i.e. in zenith direction. Assuming It can be assumed that for a given solar zenith angle the stratospheric absorption is constant for measurements at different elevation angles. Then, the differential SCD yields the integrated tropospheric concentration of a specific trace gas (for an altitude range from the surface up to about 2 to 3 km, Frieß et al., 2019, and references therein), i.e. the column density relative to the reference spectrum.

In this study, the MAX-DOAS method is used to ~~measure the NO₂~~ quantify the NO_x emissions of vehicles on a motorway. Using two MAX-DOAS instruments ~~,the~~ on the two sides of the motorway allows to measure the background NO₂ ~~DSCD is~~ DSCDs on the upwind side and additionally the traffic induced NO₂ on the downwind side. The background NO₂ DSCD is then subtracted from the ~~total~~ NO₂ DSCD on the downwind side and thus yields the NO₂ SCD caused by the traffic emissions. In a final step, the derived NO₂ SCD is converted into ~~the~~ NO_x emissions by combining it with wind data and assuming a steady state NO_x to NO₂ ratio. These steps are described in detail below.

2.1 Experimental setup

To retrieve the amount of NO_x emitted by road traffic, two Tube MAX-DOAS instruments (Donner, 2016) were set up on ~~both each~~ sides of a motorway. With these instruments, it is possible to measure the NO₂ DSCD of the ambient air along the viewing direction. The chosen measurement site is located along the heavily used A60 motorway close to Mainz, Germany, and has a long straight section which provides an advantageous geometry for the measurement setup. The exact alignment of the instruments for the presented measurement day is depicted in Fig. 1 and shows that the viewing direction is northward and parallel to the lane of traffic.

The chosen motorway section has a speed limit of 100 km h⁻¹. The next access and exit is about 1 km in one direction and 1.5 km in the other direction. Acceleration and deceleration should, therefore, only have a minor effect at the measurement site.

On the measurement day, continuous westerly wind was present so that the air mass transport was almost perpendicular to the motorway as well as to the viewing direction of the instruments. From the difference between the upwind (Instrument A, west side) and downwind (Instrument B, east side) signals, the emissions of the motorway are estimated. The locations of the instruments were about 160 m and 220 m to the west and east side of the motorway, respectively. Therefore, the area enclosed by the two Tube MAX-DOAS instruments contains the motorway section and a railway track. Possible sources of NO_x are thus traffic emissions from cars, trucks and trains ~~,since no other sources (e.g. fires) were detected in the area.~~

Measurements were taken at an elevation angle of 20° and with a total integration time of 2 s. The short integration time favours a high temporal resolution even if the quality of the spectral fit (Sect. 2.2) decreases slightly at the same time. Assuming a plume height of up to 200 m, the area of highest sensitivity can be estimated. It is also depicted in Fig. 1 by the green shading. The choice of a rather high elevation angle constrains not only the sensitivity region but also decreases the influence of variations in the background signal by reducing the light path length in the lowermost atmosphere. It should be noted that

there were broken clouds on the measurement day which possibly induce differences between the two instruments. This effect is further analysed in Sect. 2.3.

In addition, a camera and a weather station were positioned on the upwind side to obtain further information. Taking videos with this setup makes it possible to observe the traffic density on the motorway. The weather station records the wind direction and wind velocity as well as several other meteorological parameters such as pressure and temperature every second.

2.2 Spectral analysis

The spectral analysis of the obtained spectra is performed using the QDOAS software (version 2.112.2, Danckaert et al., 2012). As a reference, a series of 90° measurements were taken simultaneously with both Tube MAX-DOAS instruments at the upwind measurement site. In order to categorise differences between the two instruments (Sect. 2.3), ~~the~~ reference measurements were taken at the same location after the measurement series was completed on both sides of the motorway. The wavelength calibration is accomplished using a high resolution solar spectrum (Chance and Kurucz, 2010). For the analysis, a wavelength range of 400 nm to 460 nm was selected. The DOAS fit ~~includes trace gas absorption cross-sections (at (Vandaele et al., 1998), at (Thalman and Volkamer, 2013), at (Serdyuchenko et al., 2014), and (Rothman et al., 2010)) as well as two ring spectra, calculated with DOASIS (Kraus, 2003) using the reference spectrum, and a polynomial of 5th order also allowing an intensity offset. settings are summarised in Table 1.~~ The spectral analysis is run separately for each instrument yielding the NO₂ DSCD time series for both measurement sites. Exemplary, the QDOAS fit for one spectrum (Instrument A, upwind) is depicted in Fig. A1.

2.3 Instrumental differences

To estimate the influence of instrumental differences between the two Tube MAX-DOAS instruments on the NO₂ results, the reference spectra are investigated in more detail. These measurements were taken simultaneously with both instruments on the upwind side with an elevation angle of 90° (zenith view). Fig. 2 shows the time series of the NO₂ results for these spectra. The first 90° measurement of each instrument is taken as a reference.

As can be seen, in the grey shaded area the standard deviation between the measurements of the two instruments only amounts to

$$\Delta(\text{NO}_2 \text{ DSCD}) = 0.4 \times 10^{14} \text{ molec cm}^{-2}. \quad (2)$$

~~whereas for the~~ Hereto, the data points of instrument B were interpolated to the time axis of instrument A. For the spectra after 15:05 UTC the signal differs widely with a standard deviation of $7.9 \times 10^{14} \text{ molec cm}^{-2}$. This increased deviation is due to clouds passing by (see Sect. B1). Thus, the measurements in the grey shaded area show that both instruments measure similar NO₂ DSCDs for the same measurement conditions, i.e. the same setup, viewing direction and cloud conditions. Therefore, these spectra are being ~~integrated-accumulated~~ integrated-accumulated to minimise noise and used as fixed references which assures that both instruments are analysed under the same conditions.

2.4 Integration time

In order to investigate the influence of the integration time on the spectral analysis, the fitting procedure is performed for spectra with different integration times but the same fit settings. Therefore, two or more spectra are added before performing the DOAS fit. The result of the NO₂ retrieval as well as the average root mean square (RMS) over each measurement series is depicted in Fig. 3. The standard error of the average-mean regarding the NO₂ DSCD is about $0.006 \times 10^{16} \text{ molec cm}^{-2}$ and thus not visible in the Figure. The average-NO₂ fit error, which is given by the QDOAS analysis, shows the same trend as the average RMS. Although the average RMS-RMS. For the short integration times of our measurements, the spectral residual of the fit is dominated by photon shot noise. This is also clearly demonstrated by the observed dependence of the RMS (and the fit error) on integration time. The RMS decreases for longer integration times as the ratio of the photon shot noise to the measured signal increases. In contrast to the fit error decreasing with integration time, the NO₂ retrieval yields the same result-average NO₂ DSCDs regardless of the- for different integration times. The standard deviation between the results for different integration times amounts to less than $8 \times 10^{12} \text{ molec cm}^{-2}$ for the east side and $10 \times 10^{12} \text{ molec cm}^{-2}$ for the west side measurements which is three orders of magnitude smaller than the NO₂ signal. Consequently, the measurements taken with an integration time of 2 s give sufficient results above the detection limit which-. This is preferable as high temporal resolution is necessary to resolve specific traffic events. In the following we focus on time-averaged emissions, as for the presented measurement day no individual emission plumes could be identified. Nevertheless, it is conceivable that a detection is possible for lower traffic volume (e.g. on Sundays) or higher workload (e.g. motorway sections with higher slopes).

3 Results

3.1 Measurement results

The measurement results for ~~the~~ 10 May 2019 are shown in Fig. 4 ~~in panel (A) to (E)~~. Panel (A) depicts the time series of the measured NO₂ DSCDs for both, the upwind and downwind side, analysed as described in Sect. 2.2. The next panel (B) shows the difference between both signals

$$\text{SCD}_{\text{traffic}} = \text{DSCD}_{\text{downwind}} - \text{DSCD}_{\text{upwind}}. \quad (3)$$

A persistent offset is found with a mean value of

$$\overline{\text{SCD}}_{\text{traffic}} = \underline{(0.185 \pm 0.009)} \underline{(0.18 \pm 0.04)} \times 10^{16} \text{ molec cm}^{-2} \quad (4)$$

as represented by the orange line. The error is calculated using ~~the~~ error propagation of the standard errors of the mean for both instruments and additionally includes the deviation $\Delta(\text{NO}_2 \text{ DSCD})$ between both instruments as derived in Sect. 2.3. Moreover, an uncertainty of 16 % is added to account for the impact of the broken clouds on the measurement time series. In order to investigate the effect, a cloud filter is applied as discussed in Sect. B2.

As there are no large sources of NO₂ other than the motorway close to the measurement site, the background NO₂ DSCDs in both measurements can be assumed to be the same. Therefore, the difference between both sides is most likely due to traffic emissions. There seems to be no significant additional emission due to the passing trains (marked by the dashed grey lines in the Figure) although the railway next to the measurement site is only used by diesel trains. Temporal variations can be found in the derived difference in addition to the constant offset. ~~However, clouds have only a small impact on the measurement result as discussed in Sect. B2.~~ Panel (C) depicts the amount of traffic observed during the measurement period for which the number of vehicles was counted over one-minute intervals on a sample basis using the recorded videos. (D) ~~and (E) present the wind data presents the wind direction~~ measured by the weather station. ~~It shows the wind direction and the wind velocity at the upwind side. For (E) shows the wind velocity, also the minimum and maximum values over using a sampling rate of are depicted in grey~~ $v_{\text{wind},\perp}$ perpendicular to the viewing direction. The calculation is detailed in the next section.

3.2 Plume age

For a better understanding of the retrieved signal, the wind field needs further investigation. The quantity of interest is the wind velocity $v_{\text{wind},\perp}$ perpendicular to the viewing direction of the Tube MAX-DOAS instruments whose viewing directions are assumed to be parallel to the motorway. Thereby, the age of the measured plume can be quantified which is needed to retrieve the total emission (Sect. 3.3). The perpendicular wind velocity $v_{\text{wind},\perp}$ is shown in Fig. 4 (F) and is calculated using the measured wind velocity and the wind direction as measured by the weather station. From the alignment of the two Tube MAX-DOAS instruments as depicted in Fig. 1, it can be seen that the viewing direction corresponds to approx. 330°. The perpendicular wind velocity is thus

$$v_{\text{wind},\perp} = v_{\text{wind,meas}} \cdot \cos(\phi_{\text{wind}}) \quad (5)$$

with

$$\phi_{\text{wind}} = \phi_{\text{wind,meas}} - 330^\circ + 90^\circ, \quad (6)$$

where $\phi_{\text{wind,meas}}$ is the measured wind direction at the weather station. The error can be calculated using the propagation of uncertainty principle ~~and taking into account the~~. ~~Hereto, the error of the wind velocity is estimated using the~~ minimum and maximum values ~~of the wind data over 1 s (with a sampling rate of 4 Hz)~~. An additional error for a possible misalignment of the weather station with regard to the viewing direction of the telescopes of 2° is considered. During the measurement period, the wind velocity perpendicular to the viewing direction is at ground level on average

$$\bar{v}_{\text{wind},\perp} = (2.8 \pm 1.0) \text{ m s}^{-1}. \quad (7)$$

Effects such as turbulence, especially in the vicinity of the motorway, and changing wind fields at plume height lead to uncertainties which can, however, not be readily quantified.

Taking into account the average distance between the motorway and the downwind instrument's viewing direction $x = (195 \pm 25) \text{ m}$

estimated from Fig. 1 within the main area of high sensitivity, an average age of an air parcel of

$$t = (1.2 \pm 0.4) \text{ min} \quad (8)$$

185 can be obtained. However, variations in the wind velocity and wind direction on short time scales affect the transport of an air parcel. Therefore, the plume age cannot always be correctly represented by Eq. 8. The correlation between the wind field and the measured NO_2 SCDs is further discussed in Sect. B3. [Concluding, a constant wind velocity is favourable when applying this method.](#)

3.3 Estimation of real driving emissions

190 To estimate the real driving emissions, first the mean NO_2 SCD must be converted into a VCD using the geometric approximation as given in Eq. 1. Thus, for the elevation angle of $20 \pm 2^\circ$, [the AMF amounts to \$2.9 \pm 0.3\$ and](#) the measurement yields

$$\overline{\text{VCD}}_{\text{traffic}} = \underline{(0.63 \pm 0.07)} \underline{(0.6 \pm 0.1)} \times 10^{19} \text{ molec m}^{-2}. \quad (9)$$

195 Multiplying this value by the average wind velocity perpendicular to the viewing direction, the measured emission of NO_2 amounts to

$$E_{\text{meas, NO}_2} = (1.8 \pm 0.7) \times 10^{19} \text{ molec (m s)}^{-1}. \quad (10)$$

This value now describes the number of molecules emitted per meter and second along the motorway section. It is a direct quantity of the measurements and can be converted into emissions per vehicle per second by dividing by the number of vehicles per length of the motorway.

200 In combustion processes, N_2 is mainly oxidised into NO and in the atmosphere it is further oxidised into NO_2 and other oxides of nitrogen (Pandis and Seinfeld, 2006) forming an equilibrium between NO and NO_2 . [Especially diesel vehicles also directly emit \$\text{NO}_2\$ \(Carslaw et al., 2011, and references therein\).](#) Therefore, to retrieve the total NO_x emissions from the observed NO_2 levels, the share of NO_2 in total NO_x [at the measurement site](#) has to be known.

205 In order to estimate the rate of NO to NO_2 conversion, we used the CAABA box-model simulation with representative environment conditions and a road traffic source for the measurement period. CAABA uses the atmospheric chemistry model MECCA that includes the state of the art chemical mechanisms (Sander et al., 2019). A fraction of the traffic-emitted NO is photochemically equilibrated with air NO_2 at the daytime near-surface conditions. [Hereto, the solar radiation is calculated for clear-sky using the solar inclination at the measurement location.](#) ~~We estimate that about two-thirds of the emitted NO is thus converted into NO_2 in about 4 min. After 2 min, about 90% of the traffic-emitted NO is converted into the observed NO_2 enhancement.~~

210 One important factor regarding the conversion is the ambient ozone level, as it regulates the photochemical NO_x cycling and influences the resulting NO_2 to NO repartitioning dynamics. ~~However, our simulations with CAABA confirm that for the presented measurement the NO_2 to NO ratio is rather stable and yields a ratio of 0.7 ± 0.4 for the time $t = (1.2 \pm 0.4) \text{ min}$~~

~~which was estimated above.~~ Where the emission fluxes are very high, the titration of ozone stops further conversion of NO to NO₂. However, turbulent mixing with ambient air increases with distance from the source and ozone in the air parcel containing the plume is replenished. Thereby, the conversion of NO to NO₂ continues. Our observations confirm that, for the presented measurement, ozone titration only prevails close to the emission source and thus has no significant influence on our measurements (see Sect. C1). ~~That is due to s~~ Sufficiently high ambient ozone concentrations ~~which~~ were measured at local environmental monitoring stations (42 ppb to 44 ppb, Mainz-Mombach, distance to the measurement site approx. 5 km, and Wiesbaden-Süd, approx. 9 km, Umweltbundesamt, 2019).

The corresponding NO_x to NO₂ conversion factor, for the time $t = (1.2 \pm 0.4)$ min an air parcel needs to get from the vehicle exhaust to the sensitivity region of the Tube MAX-DOAS instrument, can be deduced to be $f = 2.4 \pm 1.0$ (Sect. C1). The NO_x emission is then derived using

$$E_{\text{meas, NO}_x} = f \cdot E_{\text{meas, NO}_2} \quad (11)$$

which equals

$$E_{\text{meas, NO}_x} = (4.3 \pm 2.5) \times 10^{19} \text{ molec (m s)}^{-1}. \quad (12)$$

In case the equilibrium is already reached, a conversion factor of $f_{\text{eq}} = 1.5$ needs to be applied instead. Then, the total NO_x emission would amount to

$$E_{\text{meas, NO}_x, \text{eq}} = (2.7 \pm 1.1) \times 10^{19} \text{ molec (m s)}^{-1}. \quad (13)$$

The determination of the conversion factor f relies on the rather rough estimate of the age of ~~the an~~ air parcel as well as the ozone concentration and chemical processes during the measurement period. Therefore, the equilibrium value gives an estimate which is independent of these factors. However, it ~~can be seen that this is is rather unlikely that the equilibrium state is reached so close to the emission source (as also found for airborne measurements of emission fluxes from power plants; Meier, 2018).~~ ~~Nonetheless, the emission value~~ $E_{\text{meas, NO}_x, \text{eq}}$ is within the error of $E_{\text{meas, NO}_x}$. In the following, the more realistic value of $E_{\text{meas, NO}_x}$ will be taken for the comparison with the expected traffic emissions.

3.4 Expected traffic emissions and comparison to real driving emissions

To calculate the expected traffic emissions, the emission per vehicle needs to be computed. The limiting values for NO_x emissions, as given by the European emission standards, are summarised in Table 2. The limiting values for passenger cars are given in NO₂ equivalents per km depending on the fuel type. For trucks, the values are reported in NO₂ equivalents per kWh. To undertake the following calculation, ~~these emission standards~~ ~~the emission standards of trucks~~ need to be converted into limiting values per km. Therefore, the values are multiplied by a conversion factor of $1.5 \pm 0.5 \text{ kWh km}^{-1}$. This is composed of the fuel value 10.4 kWh l^{-1} of diesel fuel, the efficiency of a diesel engine of about 40 % and an average consumption for trucks of 36 l per 100 km (Hilgers, 2016). The error accounts for varying fuel consumption of $\pm 10 \text{ l per 100 km}$ and the uncertainty in the efficiency of the vehicle engine.

245 The European emission standards are theoretical values for the allowed emissions of different pollutants. They are, however, not the expected emissions under real driving conditions. In order to bring the values in line, so-called Real Driving Emissions (RDE) conformity factors are used for new emission norms (Euro 6; Council of the European Union, 2016). To avoid inconsistencies, in the following only the European emission standards serve to estimate the theoretically expected emissions.

For the calculations, the statistical composition of the vehicle fleet is considered (see Table 3). The passenger car fleet is broken down by registration districts, fuel types and emission groups. To analyse the emission per vehicle, the statistical distribution of Rheinhessen-Pfalz is chosen. This also includes the city of Mainz and the Mainz-Bingen region. Note that in this area more cars with old emission standards (Euro 3 and 4) are registered compared to the average in Germany. The relative number of trucks is broken down by emission group only and relates to the distance travelled by German trucks. Attention should be paid to the fact that non-German trucks account for about 35 % of the total distance travelled in Germany (Kraftfahrt-Bundesamt, 2017).

From the emission standards and the statistical composition of the vehicle fleet, ~~the expected~~ a theoretical emission per vehicle can be calculated. The weighted average of the emission limits amount to

$$E_{\text{limit, cars}} = (116 \pm 5) \text{ mg km}^{-1} \quad (14)$$

and

260 $E_{\text{limit, trucks}} = (1248 \pm 277) \text{ mg km}^{-1} \quad (15)$

for passenger cars and trucks, respectively. The observed amount of traffic is deduced by counting the vehicles as shown in Fig. 4 and shows average values of

$$N_{\text{cars}} = (91 \pm 4) \text{ min}^{-1} \quad (16)$$

and

265 $N_{\text{trucks}} = (6 \pm 2) \text{ min}^{-1}. \quad (17)$

The error estimation accounts for miscounting the number of vehicles on the video e.g. when a truck shields the view of the other traffic lanes. Taking into account the average traffic volume, the ~~expected~~ theoretical total emission for the measuring period is given by

$$E_{\text{calc, NO}_x} = N_{\text{cars}} \cdot E_{\text{limit, cars}} + N_{\text{trucks}} \cdot E_{\text{limit, trucks}} \quad (18)$$

270 which yields

$$E_{\text{calc, NO}_x} = (0.39 \pm 0.07) (0.4 \pm 0.1) \times 10^{19} \text{ molec (m s)}^{-1}. \quad (19)$$

Here, it is used that the NO_x emissions are given in NO₂ equivalents ~~and thus~~. Thus considering the molar mass of NO₂ of 46 g mol⁻¹ (Haynes, 2014), 1 mg of NO_x emissions correspond to 1.3 × 10¹⁹ molec.

The expected-theoretical emissions calculated from the European emission standards can now be compared to the measured
275 NO_x emissions. Evidently, for 10 May 2019 the measured amount of NO_x is by a factor 11 ± 7 larger than theoretically
expected. Even if an equilibrium state between NO and NO₂ for the measured traffic emissions was assumed, the measured
NO_x emissions still show a higher value (by a factor of 7 ± 3) compared to the calculated emissions. Moreover, in the very
unlikely case that the exhaust gases primarily consist of NO₂ and the measured NO₂ difference directly equals the NO_x
emissions, this discrepancy remains unexplained. Possible error sources in the measurement cannot completely explain these
280 differences.

As the traffic volume was relatively constant throughout the measurement period, it is more likely that the statistics do not
reflect the vehicle fleet well enough and/or a large part of the vehicles does not meet the emission standards. Here, it should be
noted that the deviations of the actual vehicle composition from the assumed one cannot be the sole reason for this factor.

Assuming that only Euro 3 diesel cars and Euro III trucks, i.e. the technical status quo of the year 2000, were driving during
285 the measurement period, the expected traffic emission would amount to

$$E_{\text{calc, NO}_x, \text{Euro3/III}} = (2.0 \pm 0.5) \times 10^{19} \text{ molec (m s)}^{-1} \quad (20)$$

which is still lower than the measured emission. As today only a minor fraction of all vehicles is registered as Euro 3 cars
and Euro III trucks, this worst case scenario is highly unlikely. Considering that especially non-German trucks more often
drive with defective exhaust gas systems, these could lead to large emissions even exceeding the Euro III norm. Thereby, the
290 discrepancy between the expected-theoretical and measured emissions could be partly explained. However, trucks only account
for a small amount parts of the total traffic volume. This again implies an excess of the European emission standards regarding
NO_x emissions also for a significant number of passenger cars.

3.5 Comparison to the HBEFA database

The Handbook Emission Factors for Road Transport (HBEFA, version 4.1, Notter et al., 2019) provides emission factors for
295 all current vehicle categories as weighted average values for Germany. To draw a comparison to the results deduced in the
previous sections, the vehicle categories “passenger cars” and “heavy duty vehicles” are used as these can be readily identified
in the camera recordings of the motorway section. The aggregated emission factors for NO_x especially show higher emissions
of passenger cars as compared to the theoretical emission limits. This results in an average emission flux of

$$E_{\text{HBEFA, NO}_x} = (1.1 \pm 0.1) \times 10^{19} \text{ molec (m s)}^{-1} \quad (21)$$

300 which is roughly three times larger than expected from the European emission standards. Although the database provides
modelled real driving emissions, there remains a discrepancy to the measurements of a factor 4 ± 2. In conclusion, our
measurement method yields reasonable results and is able to quantify average emissions of the motorway section. Nonetheless,
differences remain which cannot easily be attributed to a specific error source.

4 Conclusions

305 The measurement of NO_x emissions at the A60 motorway close to Mainz, Germany, gives an estimate of ~~the~~ real driving emissions. With two MAX-DOAS instruments set up on ~~both~~ each sides of ~~the~~ a motorway, it is possible to retrieve the NO_2 signal caused by ~~the~~ road traffic and calculate the total NO_x emissions for the occurring traffic volume.

The most uncertain aspect during the analysis of the data was the age of the measured plume at the downwind side. It directly affects the conversion factor f of the NO_x to NO_2 ratio and thus the final result of the measured emission (Eq. 11). To further
310 investigate the effect of the plume age, it is favourable to set up several MAX-DOAS instruments downwind with different distances to the motorway. Thereby, the setup of the instruments could be optimised and the equilibrium state of NO_2 for the given weather conditions can be measured. Hereto, a stable wind field is advantageous. This yields a more accurate conversion factor.

Other aspects such as the high ozone concentration and relatively constant wind are uncritical for the presented measurement
315 day and allow to apply a constant conversion factor f to the average emission. Although the changing cloud cover caused large fluctuations in the NO_2 DSCDs, filtering the data leads to only slightly lower emissions. Consequently, this effect cannot explain the difference between the measured and expected emissions.

The main possible error source regarding the derivation of the expected NO_x emissions is the difference from the assumed vehicle fleet to the measured vehicle fleet. Although the statistics are relevant to the Mainz region, the exact composition
320 remains unknown. However, the worst case calculation showed that the uncertainty of the vehicle fleet cannot explain the deviation from the measured emission. Presumably, a considerable amount of vehicles did not meet the European emission standards. Moreover, it must be assumed that a substantial number of trucks are non-German vehicles. Recent studies showed that a large fraction of these vehicles had conspicuously high emissions which indicate deactivated fuel cleaning units (Pöhler and Engel, 2019). These could also explain the temporal variations in the measured time series. Applying this method at
325 different measurement sites, different driving conditions (e.g. the slope of the motorway section, the allowed speed limit, road works etc.) and the impact of the composition of the vehicle fleet could be investigated in more detail.

It can be concluded that the measured emissions on 10 May 2019 exceed the maximum expected emissions calculated from the European emission standards (Umweltbundesamt) by a factor of 11 ± 7 . The comparison to the HBEFA database also indicates elevated emissions on that motorway section. This observation is in line with the work of other groups (Carslaw
330 et al., 2011; Chen and Borcken-Kleefeld, 2014; Pöhler and Engel, 2019). Especially, the whole plume originating from the nearby motorway was measured rather than individual vehicle plumes and hence the possibility that parts of the plume get overlooked can be neglected which is a key advantage compared to other approaches such as in-situ measurements.

Data availability. Measurement data are provided in the supplement.

Appendix A

335 A1 QDOAS analysis

This section exemplary includes a fit result (Fig. A1) of the QDOAS analysis for a spectrum of Instrument A (west side, upwind) at an elevation angle of 20° using 2 s integration time. The fit settings are specified in Tab. 1.

Appendix B

B1 Effect of clouds on the reference spectra

340 Clouds can have a great impact on MAX-DOAS measurements. A change of ~~the~~ light path is caused by the increased scattering probability in clouds as there are more particles compared to the ambient air. Furthermore, the wavelength dependency of the scattered light changes for particle scattering processes compared to pure Rayleigh scattering. This effect already occurs for aerosols and is even more pronounced for clouds.

There are different methods to identify and classify clouds. Here, the temporal variation of the colour index (Wagner et al.,
345 2014) is used. The colour index (CI) is defined as the ratio of two radiance values at different wavelengths. In this case, the wavelengths 320 nm and 440 nm are chosen. Thereby, the wavelengths cover a large range to pronounce the effect of the wavelength dependency.

The CI is calculated for the 90° measurements ~~as shown in (compare to~~ Fig. 2) and the obtained temporal evolution is given in Fig. A2. ~~As for cloud free conditions a~~ An almost constant CI is expected ~~, it for cloud free conditions in this time period. It~~
350 can be seen that measurements after 15:05 UTC were affected by clouds. This leads to larger deviations in the retrieved NO₂ signal as shown in Sect. 2.3. The offset of the CI between the two instruments can be ascribed to the specific instrumental properties as the instruments are not absolutely radiometrically calibrated. Accordingly, the CI analysis also encourages the approach to use only ~~the~~ 90° measurements in the grey shaded area as a reference.

B2 Effect of clouds on the measurement result

355 Calculating the CI as described in Sect. B1 for all spectra, a characteristic behaviour can be seen (Fig. A3). As high temporal variation indicates cloud cover, all spectra where the CI is below the reference CI_{ref} are filtered. The reference was inferred by fitting a 2nd order polynomial to the data and is depicted as dashed line. The filtered time series are displayed in Fig. A4 ~~where the dashed line indicates the filter threshold~~. Recalculating the mean difference between the two measurement sites yields

$$\overline{\text{SCD}}_{\text{traffic, filtered}} = (0.156 \pm 0.009) \times 10^{16} \text{ molec cm}^{-2} \quad (\text{B1})$$

360 which is about 16 % smaller compared to the unfiltered case.

B3 Correlation to the wind field

Assuming a constant emission, the NO_2 difference is expected to be reciprocal to the wind velocity. However, an air parcel is also affected by obstacles such as trees and follows the turbulent flow of air. Furthermore, the wind varies on time scales of less than 1 min whereas the transport of the air parcel from the emission location to the sensitivity region of the MAX-DOAS instrument happens on larger time scales of 1 min or more. This means that the time of the wind measurement and the time of the NO_2 measurement are shifted by a time difference in which the wind might change strongly. Hence, the age of the air parcel cannot always be correctly represented by the simple calculation in Eq. 8. ~~In Fig. ?? the traffic emission $\text{SCD}_{\text{traffic}}$ is plotted against the inverse of the wind velocity $v_{\text{wind},\perp}^{-1}$ showing no correlation ($R^2 = 0.001 \ll 1$) between the two quantities.~~

To further test this hypothesis, both - the wind measurements and the time series of the NO_2 differences - are averaged over a time period of 12 min. Figure A5 shows a higher the correlation between both quantities ($R^2 = 0.365$). The data points are fitted using the linear least squares method (LLS, orange line) as well as using the orthogonal distance regression (ODR, green line). Here, ODR is able to take into account the standard errors of the mean values in the fitting procedure (Cantrell, 2008). In doing so, the slope of the fit increases and at the same time the intercept decreases. Comparing the fit results with the obtained emission $E_{\text{meas}, \text{NO}_2}$ over the complete NO_2 measurement series as described in Sect. 3.3, a slope of about $5000 \pm 2000 \text{ molec (m s)}^{-1}$ is expected. The fits from Figure A5 show slopes of $4230 \pm 208 \text{ molec (m s)}^{-1}$ for the LLS and $7539 \pm 2013 \text{ molec (m s)}^{-1}$ for the ODR method which are in agreement with the expected value.

Nevertheless, the weak correlation is not completely surprising because of the low variability of the wind velocity. Moreover, a constant wind velocity is generally advantageous for the measurements.

Appendix C

380 C1 CAABA-MECCA simulation

Fig. A6 presents the results of the plume emission simulation using the CAABA-MECCA box-model (Sander et al., 2019). Applying representative environmental conditions for the measurement period, road emission was approximated with a 10 s emission pulse of NO into the box. From the evolution of changes of NO and NO_2 abundances in the air parcel with time, the NO_2 to NO_x ratio of the plume is deduced.

385 To analyse the possible effect of ozone titration, a Gaussian dispersion model is applied. It uses Pasquill stability classes (Pandis and Seinfeld, 2006) based on the atmospheric stability of the measurement day. With this dispersion model, the extent of the emission plume is estimated and the NO_2 mixing ratio from our measurements is calculated. While turbulence induced by the local topography and obstacles like trees is neglected, it helps to estimate the evolution of the NO_2 mixing ratio between emission source and measurement location. From the comparison of the dispersion model and the observations, it can be

390 concluded that the ozone-poor chemical regime only prevails close to the emission source.

In order to consider this in the emission estimate calculation, the transport of the air parcel containing the plume is subdivided into two sections: 1) Close to the emission source we assume that only negligible amounts of NO are converted

395 into NO₂ and no further conversion takes place as ozone is depleted. 2) Turbulent mixing with ambient air refills the ozone reservoir and NO to NO₂ conversion can be described by the CAABA box-model simulations. For simplicity, the distance, which corresponds to the NO₂ mixing ratio matching the one simulated in the box-model, is chosen as the transition between both sections. Thereby, the time for NO to NO₂ conversion is shorter than without consideration of ozone limitations. The resulting NO_x to NO₂ ratio of the measured air parcel is estimated to be $f = 2.4 \pm 1.0$.

400 *Author contributions.* TW, SDÖ and BL designed the experiment. Adaptation of the instruments to the measurement setup was implemented by SDO, SDÖ and BL. SDÖ, BL and KU performed the measurements. SG developed and performed the simulations. BL prepared the manuscript with contributions from all co-authors. TW, SB, SDÖ and SDO contributed with valuable feedback and supervised the study.

Competing interests. The authors declare that they have no conflicts of interests.

405 *Acknowledgements.* We acknowledge the electronics workshop (i.e. Thomas Klimach, Christian Gurk, Mark Lamneck and Frank Helleis) and the mechanical workshop (i.e. Michael Dietrich and Ralf Wittkowski) of the Max-Planck Institute for Chemistry, Mainz, for the continuous support in the development of the Tube MAX-DOAS instrument. We are also thankful to Denis Pöhler (Airyx GmbH) for sharing his expertise on traffic emission estimation.

References

- Borgeest, K.: Manipulation von Abgaswerten: Technische, gesundheitliche, rechtliche und politische Hintergründe des Abgasskandals, Springer-Verlag, <https://doi.org/10.1007/978-3-658-17181-0>, 2017.
- 410 Cantrell, C. A.: Technical Note: Review of methods for linear least-squares fitting of data and application to atmospheric chemistry problems, *Atmospheric Chemistry and Physics*, 8, 5477–5487, <https://doi.org/10.5194/acp-8-5477-2008>, 2008.
- Carslaw, D. C., Beevers, S. D., Tate, J. E., Westmoreland, E. J., and Williams, M. L.: Recent evidence concerning higher NO_x emissions from passenger cars and light duty vehicles, *Atmospheric Environment*, 45, 7053–7063, <https://doi.org/10.1016/j.atmosenv.2011.09.063>, 2011.
- 415 Chance, K. and Kurucz, R. L.: An improved high-resolution solar reference spectrum for earth's atmosphere measurements in the ultraviolet, visible, and near infrared, *Journal of quantitative spectroscopy and radiative transfer*, 111, 1289–1295, <https://doi.org/10.1016/j.jqsrt.2010.01.036>, 2010.
- Chen, Y. and Borken-Kleefeld, J.: Real-driving emissions from cars and light commercial vehicles—Results from 13 years remote sensing at Zurich/CH, *Atmospheric Environment*, 88, 157–164, <https://doi.org/10.1016/j.atmosenv.2014.01.0400>, 2014.
- 420 Council of the European Union: Commission Regulation (EU) 2016/427 of 10 March 2016 amending Regulation (EC) No 692/2008 as regards emissions from light passenger and commercial vehicles (Euro 6), OJ L, 82, 1–98, 2016.
- Council of the European Union: Commission Regulation (EU) 2017/1151 of 1 June 2017 supplementing Regulation (EC) No 715/2007 of the European Parliament and of the Council on type-approval of motor vehicles with respect to emissions from light passenger cars and commercial vehicles (Euro 5 and Euro 6), OJ L, 175, 1–643, 2017.
- 425 Danckaert, T., Fayt, C., Van Roozendael, M., De Smedt, I., Letocart, V., Merlaud, A., and Pinaridi, G.: QDOAS Software user manual, 2012.
- Donner, S.: Mobile MAX-DOAS measurements of the tropospheric formaldehyde column in the Rhein-Main region, Master's thesis, University of Mainz, <http://hdl.handle.net/11858/00-001M-0000-002C-EB17-2>, 2016.
- European Parliament and Council of the European Union: 70/220/EEC of 20 March 1970 on the approximation of the laws of the Member States relating to measures to be taken against air pollution by gases from positive-ignition engines of motor vehicles, OJ L, 76, 1–22, 1970.
- 430 European Parliament and Council of the European Union: 98/69/EC of the European Parliament and of the Council of 13 October 1998 relating to measures to be taken against air pollution by emissions from motor vehicles and amending Council Directive 70/220/EEC, OJ L, 350, 12, 1998.
- European Parliament and Council of the European Union: Regulation (EC) No 715/2007 of the European Parliament and of the Council of 20 June 2007 on type approval of motor vehicles with respect to emissions from light passenger and commercial vehicles (Euro 5 and 435 Euro 6) and on access to vehicle repair and maintenance information., OJ L, 171, 1–16, 2007.
- European Parliament and Council of the European Union: Council Directive 2008/50/EC on ambient air and cleaner air for Europe, OJ L, 151, 1–44, 2008.
- 440 Frieß, U., Beirle, S., Alvarado Bonilla, L., Bösch, T., Friedrich, M. M., Hendrick, F., Piders, A., Richter, A., van Roozendael, M., Rozanov, V. V., Spinei, E., Tirpitz, J.-L., Vlemmix, T., Wagner, T., and Wang, Y.: Intercomparison of MAX-DOAS vertical profile retrieval algorithms: studies using synthetic data, *Atmospheric Measurement Techniques*, 12, 2155–2181, <https://doi.org/10.5194/amt-12-2155-2019>, 2019.

- © Google Earth Pro: Mainz, 49°58'55.48"N 8°12'34.81"E, eye altitude 4.98 km.
Google 2018, GeoBasis-DE/BKG 2009., 2018.
- Haynes, W. M.: CRC handbook of chemistry and physics, CRC press, 2014.
- 445 Hilgers, M.: Kraftstoffverbrauch und Verbrauchsoptimierung, Springer, <https://doi.org/10.1007/978-3-658-12751-00>, 2016.
- Hönninger, G., Friedeburg, C. v., and Platt, U.: Multi axis differential optical absorption spectroscopy (MAX-DOAS), *Atmospheric Chemistry and Physics*, 4, 231–254, <https://doi.org/10.5194/acp-4-231-20040>, 2004.
- IPCC: Climate Change 2013: The Physical Science Basis. Contribution of Working Group I to the Fifth Assessment Report of the Intergovernmental Panel on Climate Change, Cambridge, UK and New York, New York, USA, 2013.
- 450 Kraftfahrt-Bundesamt: Lastfahrten im Inlandsverkehr nach Hauptverkehrsbeziehungen mit europäischen Lastkraftfahrzeugen im Jahr 2017, https://www.kba.de/DE/Statistik/Kraftverkehr/europaeischerLastkraftfahrzeuge/Inlandsverkehr/inlandsverkehr_node.html, last accessed: 18.07.2019, 2017.
- Kraftfahrt-Bundesamt: FZ 1 Bestand an Kraftfahrzeugen und Kraftfahrzeuganhängern nach Zulassungsbezirken, 1. Januar 2019, <https://www.kba.de>, last accessed: 26.02.2020, 2019a.
- 455 Kraftfahrt-Bundesamt: VD 5 Verkehr deutscher Lastkraftfahrzeuge Gesamtverkehr März 2019, <https://www.kba.de>, last accessed: 19.02.2020, 2019b.
- Kraus, S.: DOAS Intelligent System, institute of Environmental Physics, University of Heidelberg, Cooperation with Hoffmann Messtechnik GmbH, 2003.
- Meier, A. C.: Measurements of horizontal trace gas distributions using airborne imaging differential optical absorption spectroscopy, Ph.D. thesis, Universität Bremen, 2018.
- 460 Notter, B., Keller, M., Althaus, H.-J., Cox, B., Knörr, W., Heidt, C., Biemann, K., Räder, D., and Jamet, M.: HBEFA (Handbook Emission Factors for Road Transport) 4.1 Development Report, <https://www.hbefa.net/e/index.html>, online version, Last accessed: 18.08.2020, 2019.
- Pandis, S. N. and Seinfeld, J. H.: Atmospheric chemistry and physics: From air pollution to climate change, Wiley, 2006.
- 465 Platt, U. and Stutz, J.: Differential Optical Absorption Spectroscopy: Principles and Applications, Springer Science & Business Media, 2008.
- Pöhler, D. and Engel, T.: Bestimmung von realen Lkw NO_x-Emissionen (Real Driving Emissions) und hohen Emittlern auf deutschen Autobahnen, 2019.
- Rothman, L., Gordon, I., Barber, R., Dothe, H., Gamache, R., Goldman, A., Perevalov, V., Tashkun, S., and Tennyson, J.: HITEMP, the high-temperature molecular spectroscopic database, *Journal of Quantitative Spectroscopy and Radiative Transfer*, 111, 2139–2150, <https://doi.org/10.1016/j.jqsrt.2010.05.001>, 2010.
- 470 Sander, R., Baumgaertner, A., Cabrera-Perez, D., Frank, F., Gromov, S., Groß, J.-U., Harder, H., Huijnen, V., Jöckel, P., Karydis, V. A., et al.: The community atmospheric chemistry box model CAABA/MECCA-4.0, *Geoscientific model development*, 12, 1365–1385, <https://doi.org/10.5194/gmd-12-1365-20190>, 2019.
- Serdyuchenko, A., Gorshchev, V., Weber, M., Chehade, W., and Burrows, J.: High spectral resolution ozone absorption cross-sections—Part 2: Temperature dependence, *Atmospheric Measurement Techniques*, 7, 625–636, <https://doi.org/10.5194/amt-7-625-20140>, 2014.
- Thalman, R. and Volkamer, R.: Temperature dependent absorption cross-sections of O₂–O₂ collision pairs between 340 and 630 nm and at atmospherically relevant pressure, *Physical chemistry chemical physics*, 15, 15 371–15 381, <https://doi.org/10.1039/C3CP50968K>, 2013.
- Umweltbundesamt: Emissionsstandards, <https://www.umweltbundesamt.de/themen/verkehr-laerm/emissionsstandards>, last accessed: 06.07.2019.

- 480 Umweltbundesamt: Aktuelle Luftdaten, Fachgebiet II 4.2, Beurteilung der Luftqualität, <https://www.umweltbundesamt.de/daten/luftbelastung/aktuelle-luftdaten>, ozone concentration of 10 May 2019 at Mainz-Mombach (DERP007) and Wiesbaden-Süd (DEHE022), 2019.
- Vandaele, A. C., Hermans, C., Simon, P. C., Carleer, M., Colin, R., Fally, S., Merienne, M.-F., Jenouvrier, A., and Coquart, B.: Measurements of the NO₂ absorption cross-section from 42 000 cm⁻¹ to 10 000 cm⁻¹ (238–1000 nm) at 220 K and 294 K, *Journal of Quantitative Spectroscopy and Radiative Transfer*, 59, 171–184, 1998.
- 485 Wagner, T., Apituley, A., Beirle, S., Dörner, S., Friess, U., Remmers, J., and Shaiganfar, R.: Cloud detection and classification based on MAX-DOAS observations, *Atmospheric Measurement Techniques*, 7, 1289–1320, <https://doi.org/10.5194/amt-7-1289-2014>, 2014.
- World Health Organization et al.: Air quality guidelines for Europe, 2000.

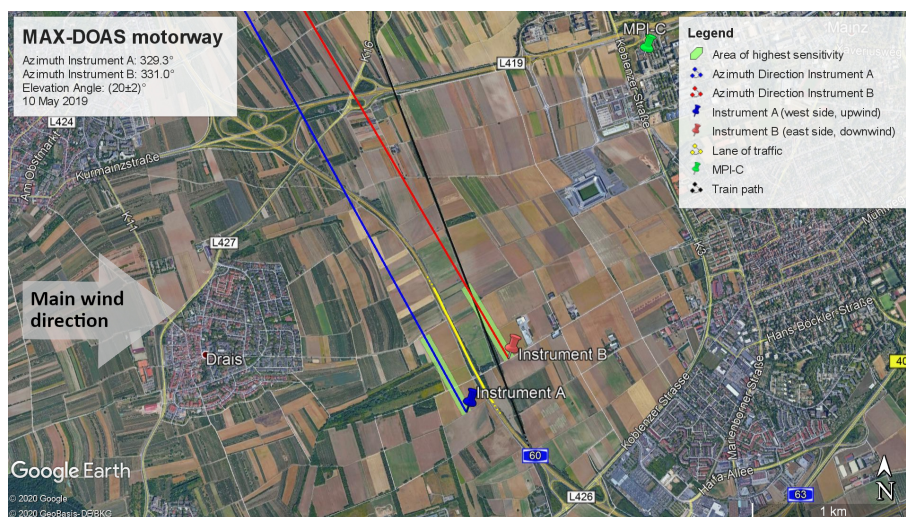


Figure 1. Alignment of the two Tube MAX-DOAS instruments on the measurement day, 10 May 2019. The instruments are located on both sides of the A60 motorway, Mainz, Germany, with a viewing direction parallel to the lane of traffic. The area between both instruments encloses the motorway and the railway track. Our measurements have highest sensitivity within the green shaded area. On the measurement day, continuous wind from westerly directions was present. Created with © Google Earth Pro (2018).

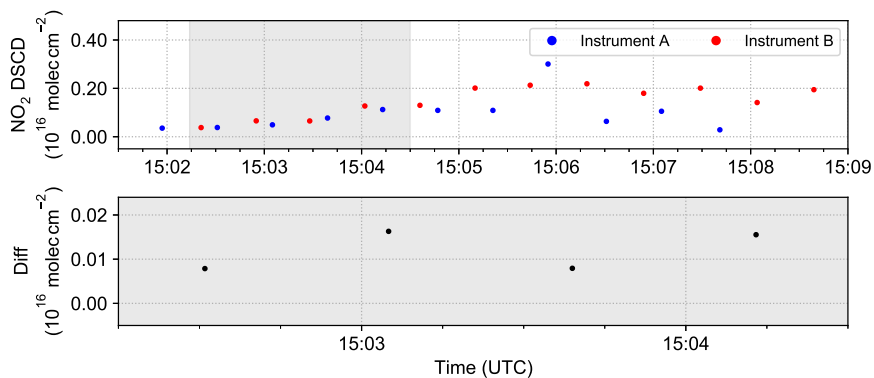


Figure 2. Time series of the NO₂ results for the 90° measurements of both instruments on the upwind side. **In the upper panel the label refers to the place of each instrument during the measurement of the traffic emissions.** The spectra are analysed using the first 90° spectrum as a reference. **The grey shaded area denotes the range where both measured similar NO₂ DSCDs.** In the lower panel the difference between the two Tube MAX-DOAS instruments is depicted. **The , zoomed into the grey shaded area denotes the range where both measured similar DSCDs.**

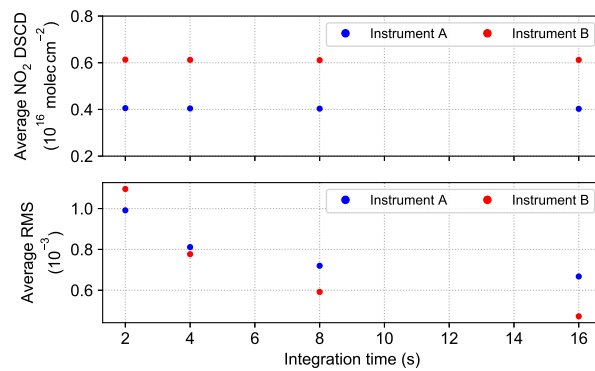


Figure 3. Average NO₂ DSCD and average RMS for both measurement sites (blue Instrument A: west side, upwind; red Instrument B: east side, downwind) for different integration times.

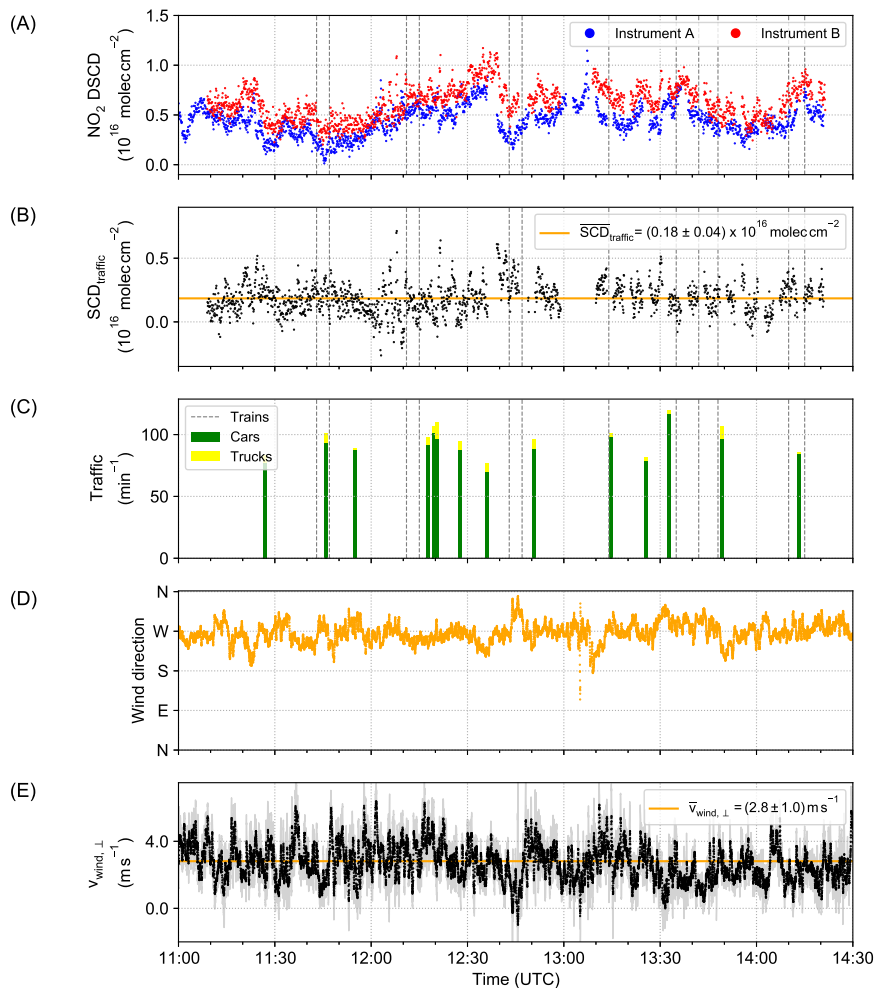


Figure 4. Time series of the measurement results of the 10 May 2019. (A) depicts the measured NO₂ DSCD for both measurement sites (blue Instrument A: west side, upwind; red Instrument B: east side, downwind). In (B) the difference SCD_{traffic} between both signals is shown. The orange line symbolises the average value. (C) presents the traffic volume during the measuring duration. The number of vehicles was retrieved by counting from the videos over one-minute intervals on a sample basis. The dashed grey lines represent the times of passing trains. (D) and (E) depict depicts the wind direction and wind velocity as measured by the weather station at the upwind side. The light grey values in (E) show the minimum and maximum wind velocities. (F) shows the wind velocity $v_{\text{wind},\perp}$ perpendicular to the viewing direction of the Tube MAX-DOAS instruments. The orange line denotes the mean value over the whole measurement period. Here, the light grey values depict the error $\Delta v_{\text{wind},\perp}$ of the calculated wind velocity.

Table 1. Settings of the spectral analysis.

<u>Species</u>	<u>Cross-section</u>
<u>NO₂</u>	<u>Vandaele et al. (1998), @ 298 K</u>
<u>O₄</u>	<u>Thalman and Volkamer (2013), @ 293 K</u>
<u>O₃</u>	<u>Serdyuchenko et al. (2014), @ 223 K</u>
<u>H₂O</u>	<u>Rothman et al. (2010), HITEMP</u>
<u>Ring, Second Ring</u>	<u>Calculated with DOASIS (Kraus, 2003) using the reference spectrum</u>
<u>Polynomial</u>	<u>5th order</u>
<u>Offset</u>	<u>constant</u>

Table 2. European emission standards for NO_x emissions (Umweltbundesamt).

For passenger cars separated into fuel types
in mg km⁻¹ NO₂:

	Euro 3	Euro 4	Euro 5	Euro 6
diesel	500	250	180	80
petrol	150	80	60	60

For trucks in mg kWh⁻¹ NO₂:

Euro III	Euro IV	Euro V	Euro VI
5000	3500	2000	460

Table 3. Vehicle fleet composition by emission group in %.

For passenger cars (Kraftfahrt-Bundesamt, 2019a):				
	Euro 3	Euro 4	Euro 5	Euro 6
diesel	3±1	6±1	11±1	8±1
petrol	6±1	23±1	16±1	16±1

For trucks (Kraftfahrt-Bundesamt, 2019b):				
	Euro III	Euro IV	Euro V	Euro VI
	1±1	1±1	19±1	78±1

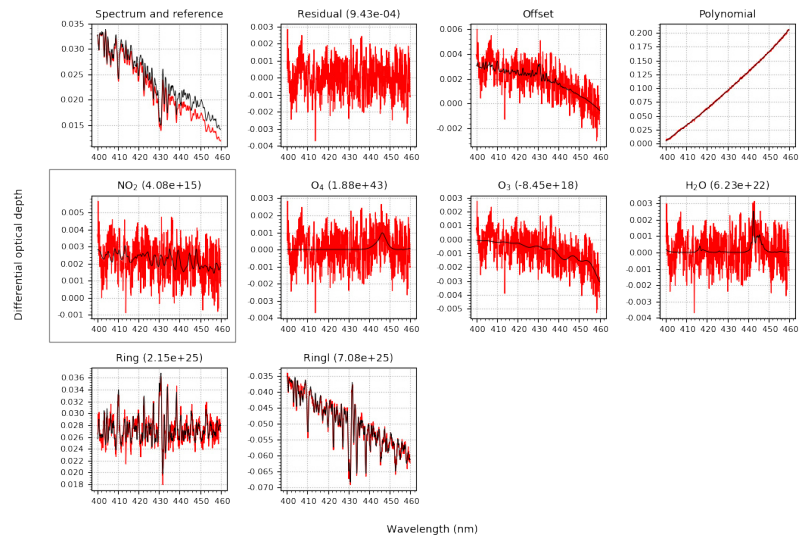


Figure A1. Example fit result of the QDOAS analysis (Instrument A: west side, upwind; 11:59:11 UTC, 10 May 2019). The measured optical densities of different absorbers are depicted in red whereas the fit results are depicted in black. The values in the titles refer to the resulting slant column densities in molec cm².

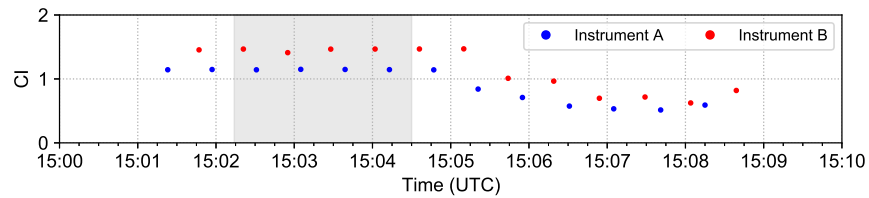


Figure A2. The temporal evolution of the colour index (CI, [intensity ratio 320 nm/440 nm](#)) for the 90° measurements, which were taken simultaneously at the upwind side, is depicted. ~~The label refers to the place of each instrument during the measurement of the traffic emissions.~~ The grey shaded area depicts the range where both instruments measured the same NO₂ signal (compare to Fig. 2).

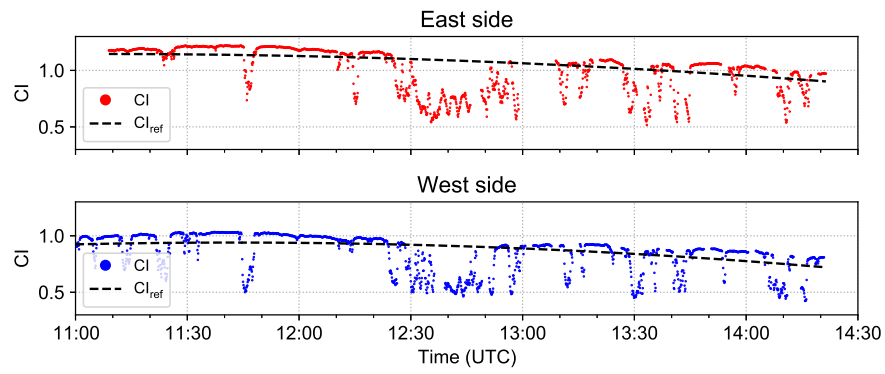


Figure A3. The colour index (CI, intensity ratio 320 nm/440 nm) for both measurement series. The dashed line (CI_{ref}) indicates the filter threshold.

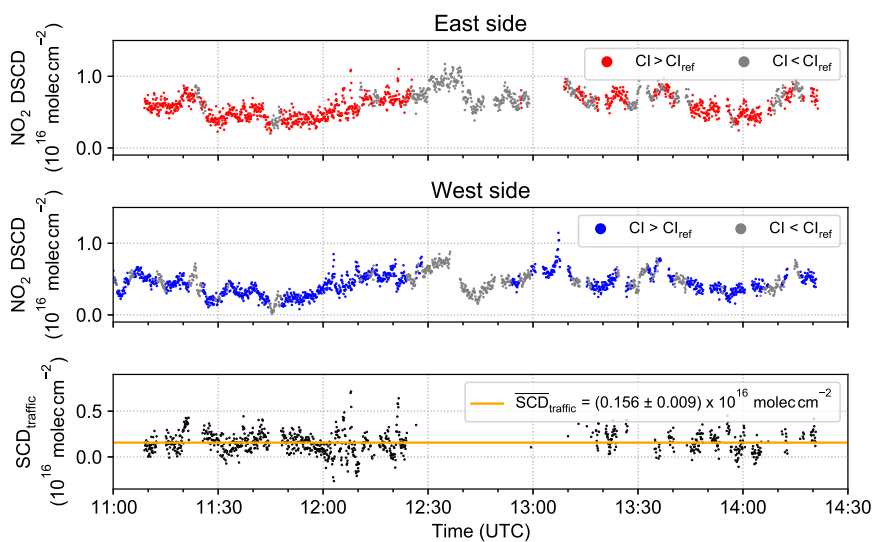


Figure A4. Analysis result of the NO₂ DSCDs for both sides (blue: west side, upwind; red: east side, downwind) with applied cloud filter based on the colour index (CI, [intensity ratio 320 nm/440 nm](#)). The grey data points are filtered out. The resulting difference SCD_{traffic} is depicted in the lowermost panel yielding slightly lower NO₂ SCDs compared to the unfiltered case.

490 Correlation between the inverse of the wind velocity $v_{\text{wind},\perp}^{-1}$ perpendicular to the viewing direction of the Tube-MAX-DOAS instruments and the signal $\text{SCD}_{\text{traffic}}$ with a linear least squares (LLS) fit.

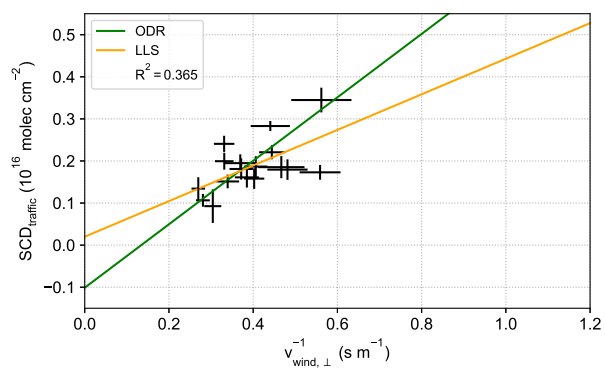


Figure A5. Correlation between the inverse of the wind velocity $v_{\text{wind},\perp}^{-1}$ perpendicular to the viewing direction of the Tube MAX-DOAS instruments and the NO₂ signal $\text{SCD}_{\text{traffic}}$ for a 12 min averaging time span. The data points were fitted using the linear least squares method (LLS) and orthogonal distance regression (ODR).

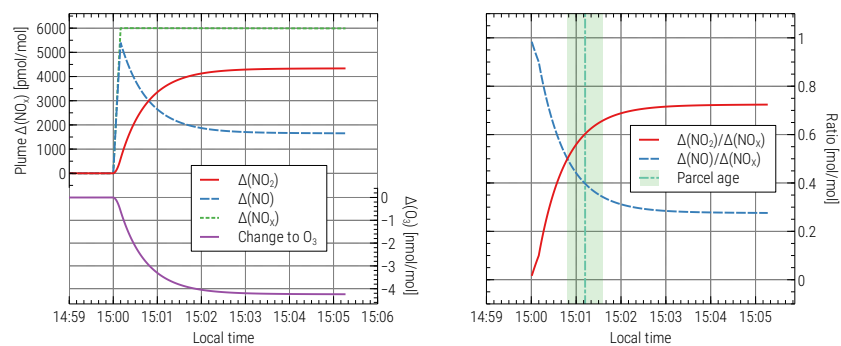


Figure A6. CAABA-MECCA box-model simulation for the presented measurement day using representative environmental conditions. At 15:00 simulated local time, a 10 s emission of NO into the box is performed representing the emission from road traffic. The left panel shows changes of $\text{NO}_x = \text{NO} + \text{NO}_2$ and ozone (O_3) compared to the background values. The right panel depicts the NO_2 to NO_x as well as NO to NO_x ratio in the plume.